

Supporting Information

Exploring the existing drug space for Novel pTyr Mimetic and SHP2 Inhibitors

Rongjun He,^{†,#} Zhi-Hong Yu,^{†,#} Ruo-Yu Zhang,[†] Li Wu,[‡] Andrea M. Gunawan,[‡] Brandon S. Lane,[†] Joong S. Shim,[§] Li-Fan Zeng,[†] Yantao He,[†] Lan Chen,[‡] Clark D. Wells,[†] Jun O. Liu,[§] and Zhong-Yin Zhang^{*,†,‡}

[†]Department of Biochemistry and Molecular Biology, [‡]Chemical Genomics Core Facility, Indiana University School of Medicine, 635 Barnhill Drive, Indianapolis, IN 46202, United States

[§]Department of Pharmacology & Molecular Sciences, Johns Hopkins University School of Medicine, 725 N Wolfe Street, Baltimore, MD 21205, United States

[#]These authors contributed equally to this work

Index

1. Figure S1: Lineweaver-Burk plot for SHP2 inhibition by cefsulodin	Page 2
2. Cefsulodin is a reversible SHP2 inhibitor	Page 3
3. Figure S2: LC-MS characterization of SHP2 inhibition by cefsulodin	Page 4
4. Figure S3: QTOF-MS characterization of SHP2 inhibition by cefsulodin	Page 5
5. Table S1: Data collection and structure refinement statistics	Page 6
6. Structural and mass spectrometry analyses of the SHP2•compound 1 adduct	Page 7
7. Figure S4: Compound 1 is covalently bonded with SHP2 under crystallization state	Page 8
8. Figure S5: Stability of cefsulodin under various conditions	Page 9
9. Figure S6: ESI-MS data of cefsulodin with buffer components	Page 11
10. Figure S7: Chemical structures of a set of 192 amines	Page 12
11. NMR spectra of Lib-1 to Lib-4 , and compounds 2 to 5	Page 13
12. LC-MS spectra of Lib-1 to Lib-4 , and compounds 2 to 5	Page 26
13. Experimental Procedures	
Protein expression and purification	Page 34
Enzyme kinetics and inhibition studies	Page 34
Characterization of cefsulodin-mediated SHP2 inhibition	Page 35
X-Ray Crystallography studies	Page 36
Chemical synthesis	Page 36
Cell proliferation and immunoblot analysis	Page 39
Effects of compound 2 on cell growth in Matrigel	Page 40
14. References	Page 41

1. Figure S1

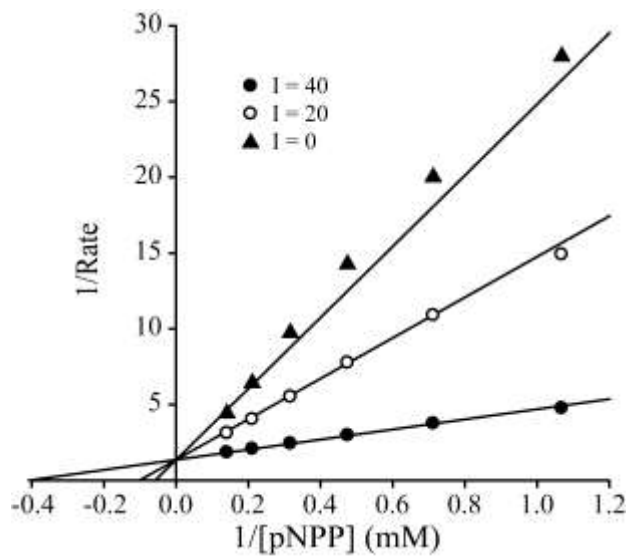


Figure S1. Lineweaver-Burk plot for Cefsulodin mediated SHP2 inhibition. Cefsulodin is a competitive inhibitor of SHP2 with K_i at $6.6 \mu\text{M}$. Cefsulodin concentrations were 0 (\blacktriangle), 20 (\circ) and 40 (\bullet) μM .

2. Cefsulodin is a reversible SHP2 inhibitor.

Since the PTP-catalyzed reaction employs nucleophilic catalysis,¹ we determined whether cefsulodin acts as an irreversible inhibitor and inactivates SHP2 by a covalent mechanism. To this end, we re-measured the IC_{50} of cefsulodin against SHP2 under the same assay conditions by either incubating cefsulodin with SHP2 for 30 min prior to the addition of *p*NPP, or incubating cefsulodin with *p*NPP for 30 min prior to the addition of SHP2. Reversible and fast-binding inhibitors are not expected to display time dependency whereas irreversible or tight-binding inhibitors will exhibit significantly reduced IC_{50} values when they are pre-incubated with the enzyme. Similar IC_{50} values were obtained for cefsulodin under both conditions (cefsulodin pre-mixed with SHP2, $IC_{50} = 16.8 \pm 1.8 \mu\text{M}$; cefsulodin pre-mixed with *p*NPP, $IC_{50} = 17.5 \pm 2.0 \mu\text{M}$), suggesting that cefsulodin does not inactivate SHP2, at least not within the duration of the assay time. We also monitored SHP2-catalyzed *p*NPP hydrolysis in the presence of cefsulodin by LC-MS as a function of time at the same pH and temperature (Figure S2). No evidence of SHP2 modification was observed and no change in cefsulodin concentration was evident. Finally, we incubated SHP2 (100 nM and 10 μM) with 100 μM cefsulodin for three hours and found no covalent adduct formation between SHP2 and cefsulodin (Figure S3B and S3C). As a positive control, phenyl vinyl sulfone, a known PTP activity-based probe that covalently modifies the catalytic cysteine,² formed a covalent adduct with SHP2 within 10 minutes (Figure S3D). Taken together, these studies indicated that cefsulodin is a competitive and reversible SHP2 inhibitor.

3. Figure S2

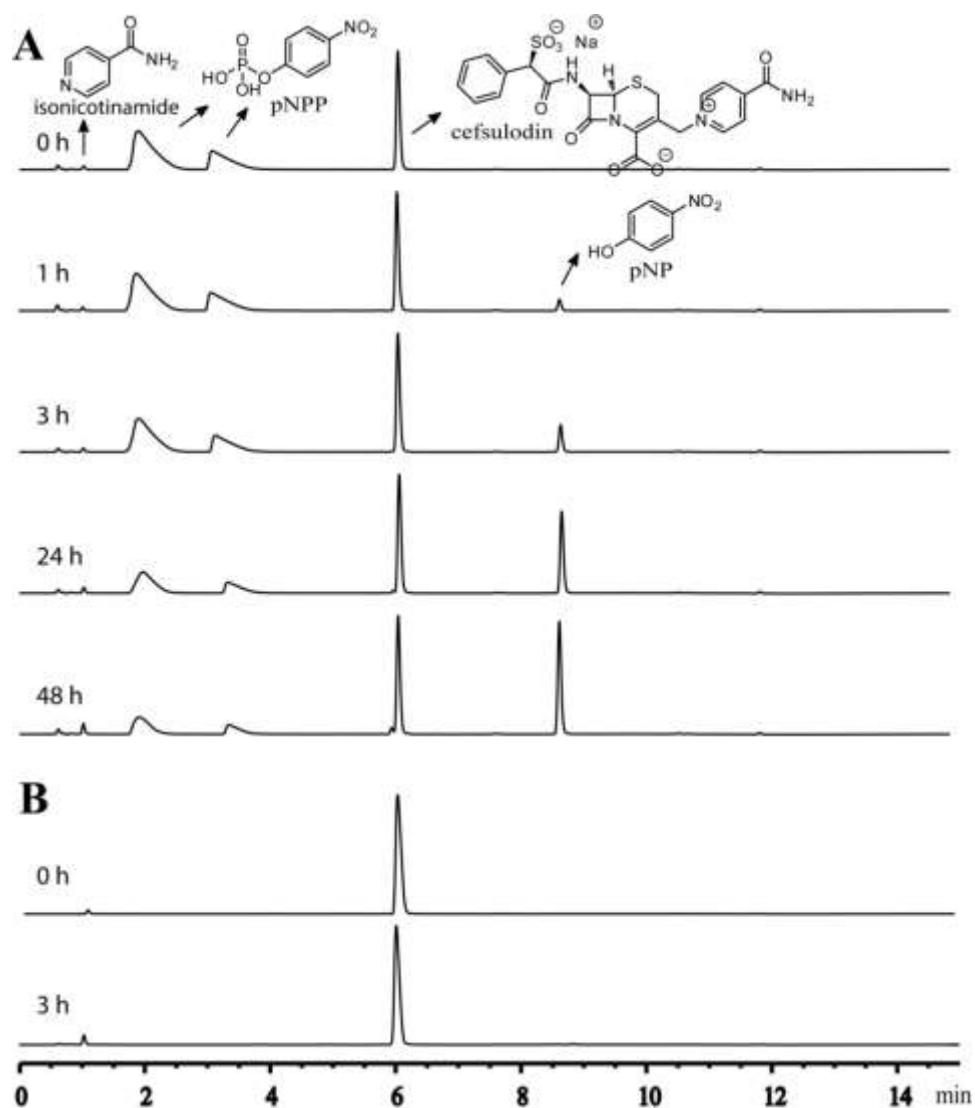


Figure S2. LC-MS characterization of SHP2 inhibition by cefsulodin. **A)** Under inhibition assay conditions (pH 7 and 25 °C, 20 nM SHP2, 3 mM *p*NPP, 100 μ M cefsulodin, 50 mM 3,3-dimethylglutarate and 1 mM EDTA with an ionic strength of 0.15 M adjusted by addition of NaCl, total volume 200 μ L), the reaction mixture was monitored at UV absorbance at 254 nm and analyzed by LC-MS at time points of 0 h, 3 h, 24 h and 48 h. LC-MS spectra at various time points showed no change in cefsulodin (retention time 6.1 min) and isonicotinamide (retention time 1.0 min, a marker of cefsulodin degradation) concentrations, while the level of *p*NPP (retention time 2.0 and 3.5 min) decreased progressively with concurrent increase of its hydrolyzed product *p*-nitrophenol (retention time 8.6 min), indicating SHP2 is active throughout the 48 hours. **B)** Incubation with cefsulodin at a higher concentration of SHP2 (10 μ M) under the same conditions for 3 hours showed no cefsulodin degradation, indicating cefsulodin is not reacting with SHP2.

4. Figure S3

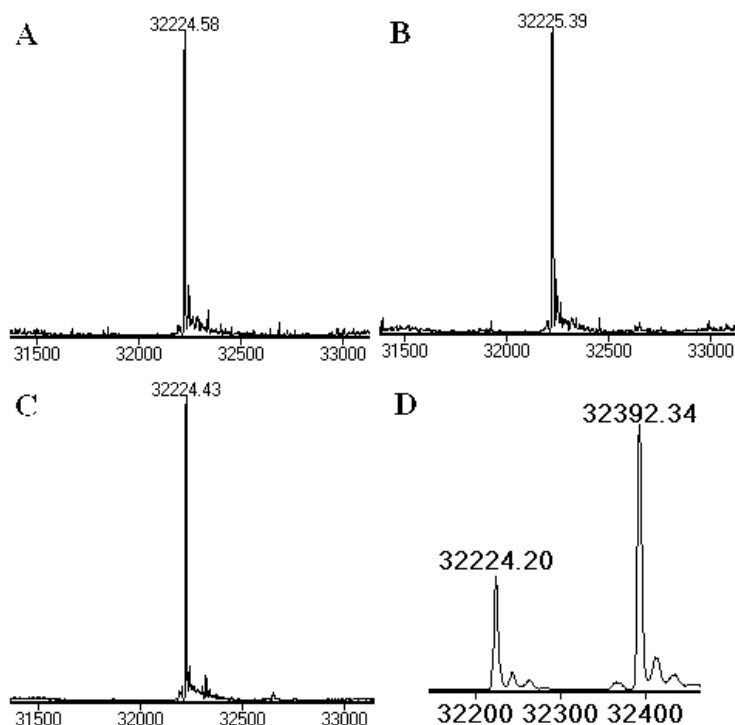


Figure S3. QTOF-MS characterization of SHP2 inhibition by cefsulodin under assay conditions. **A)** ESI-MS analysis of SHP2 indicated that it has a molecular weight of 32224.58. **B)** After incubation of cefsulodin (100 μ M) and SHP2 (100 nM) in 50 mM 3,3-dimethylglutarate and 1 mM EDTA with an ionic strength of 0.15 M (pH=7.0) for 3 h, ESI-MS analysis showed only one peak at 32225.39. **C)** After incubation of cefsulodin (100 μ M) and SHP2 (10 μ M) in 50 mM 3,3-dimethylglutarate and 1 mM EDTA with an ionic strength of 0.15 M (pH=7.0) for 3 h, ESI-MS analysis again showed only one peak at 32224.43. **D)** After incubation of phenyl vinyl sulfone (PVS) (100 μ M) and SHP2 (100 nM) in 50 mM 3,3-dimethylglutarate and 1 mM EDTA with an ionic strength of 0.15 M (pH 7) for 10 min, ESI-MS analysis showed the unmodified SHP2 peak at 32224.20 and SHP2•PVS covalent adduct at 32392.34. PVS has a molecular mass of 168.21.

5. Table S1. Data collection and structure refinement statistics.

SHP2•Compound 1	
Data collection	
Space group	<i>P2</i> ₁
Cell dimensions □ □ □	
a, b, c (Å)	39.64, 75.27, 48.05
α, β, γ (°)	90.0, 99.1, 90.0
Resolution (Å)	1.60 (1.63-1.60)
<i>R</i> _{merge}	0.077 (0.666)
<i>I</i> / σ <i>I</i>	22.1 (1.5)
Completeness (%)	97.3 (80.0)
Redundancy	3.4 (2.7)
Refinement	
Resolution (Å)	1.60
No. reflections	35,592
<i>R</i> _{work} / <i>R</i> _{free}	0.175 / 0.201
No. atoms	
Protein	2,151
Ligand	28
Water	368
R.m.s. deviations	
Bond lengths (Å)	0.007
Bond angles (°)	1.098
Ramachandran plot (%)	
Most favored regions	90.4
Additional allowed regions	8.8
Generously allowed regions	0.8
Disallowed regions	0

The dataset was collected from a single crystal. Values in parentheses are for highest-resolution shell.

6. Structural and mass spectrometry analyses of the SHP2-compound 1 adduct

Further inspection of the 2Fo-Fc map at 0.76 revealed weak electron density extending from X (Figure S4A) to a space occupied by a flexible loop (residues 314 to 324, which have not been observed in all previously reported SHP2 structures) from a symmetry-related SHP2 molecule. This promoted us to investigate whether a covalent bond was formed between compound 1 and SHP2. Thus crystals of SHP2, as well as co-crystals of SHP2•cefsulodin complex were collected respectively, washed and re-dissolved in water, and the resulting solution was subjected to QTOF ESI-MS analysis. As shown in Figure S4B, the re-dissolved apo-SHP2 crystals show only one peak at 32224.57, which corresponds to the molecular mass of the SHP2 catalytic domain (residue 262-528). In contrast, the re-dissolved co-crystals of SHP2•cefsulodin has an additional peak at 32652.80 (Figure S4C), and the difference between these two peaks is 428.24, which corresponds to the molecular mass of compound 1 minus two hydrogen atoms, likely as a result of covalent bond formation with SHP2. To identify the residue covalently attached to compound 1, we re-constructed the missing loop (residue 314 to 324) based on the 2Fo-Fc electron density observed at 0.76 through iterative cycles of building and refinement (Figure S4D). Through crystallographic symmetry operations, X was found to overlap nicely with the sulfur atom in C318 from the flexible loop in a symmetry-related SHP2 molecule (Figure S4E), and the 2Fo-Fc electron density at 0.76 accounts well for compound 1 covalently attached to C318 (Figure S4F), supporting the existence of a covalent bond between the SHP2 active site bound compound 1 and a symmetry-related SHP2 molecule in the co-crystal (Figure S4E).

How can one reconcile the apparent contradictory findings that cefsulodin acts as a reversible and competitive SHP2 inhibitor in assay solution but forms a covalent adduct with SHP2 in the crystalline state? One plausible explanation may be that cefsulodin covalently modifies SHP2 during the crystallization process. Cefsulodin is most stable under pH 4-6 but readily degrades when the pH is over 7, a process which could be accelerated by the presence of strong nucleophiles.³ There are two reactive sites in cefsulodin (β -lactam core and isonicotinamide),^{4, 5} and the loss of isonicotinamide precedes β -lactam ring opening due to higher reactivity.⁶ Consistent with previous reports that cefsulodin stability is highly pH dependent, degradation of cefsulodin was negligible when monitored in pH 5.8 MES buffer (20 mM MES, 250 mM NaCl, 1 mM EDTA) (Figure S5B). In contrast, cefsulodin degradation was obvious in pH 7.4 CBTP buffer (33 mM Citric acid, 67 mM BIS-TRIS Propane) and its degradation was further accelerated in CBTP buffer at pH 9.1 (Figure S5C and S5D).

In the crystallization experiment, the MES (pH 5.8) buffer containing 0.2 mM SHP2, 1 mM cefsulodin and 2 mM DTT was mixed with an equal volume of the CBTP buffer (pH 7.4), and the resulting solution (final pH=7.1) was allowed to stand at 20 °C for several days. Under this condition, cefsulodin was completely degraded within 2 days (Figure S5E). In addition, conjugate adducts of cefsulodin with either CBTP (Figure S6A and S6C) or DTT (Figure S6B and S6D) could be detected in the cefsulodin samples stored in the pH 7.4 CBTP buffer and under crystallization conditions. Given the proximity of C318 to the isonicotinamide group in the crystal, it is reasonable to speculate that upon cefsulodin binding to SHP2 active site in the crystalline state, the isonicotinamide tail in cefsulodin is poised to be replaced by C318 from a nearby symmetry-related SHP2 molecule, and the β -lactam ring is subsequently opened by water to form the SHP2-compound 1 adduct as observed in the crystal structure (Figure S4E).

7. Figure S4

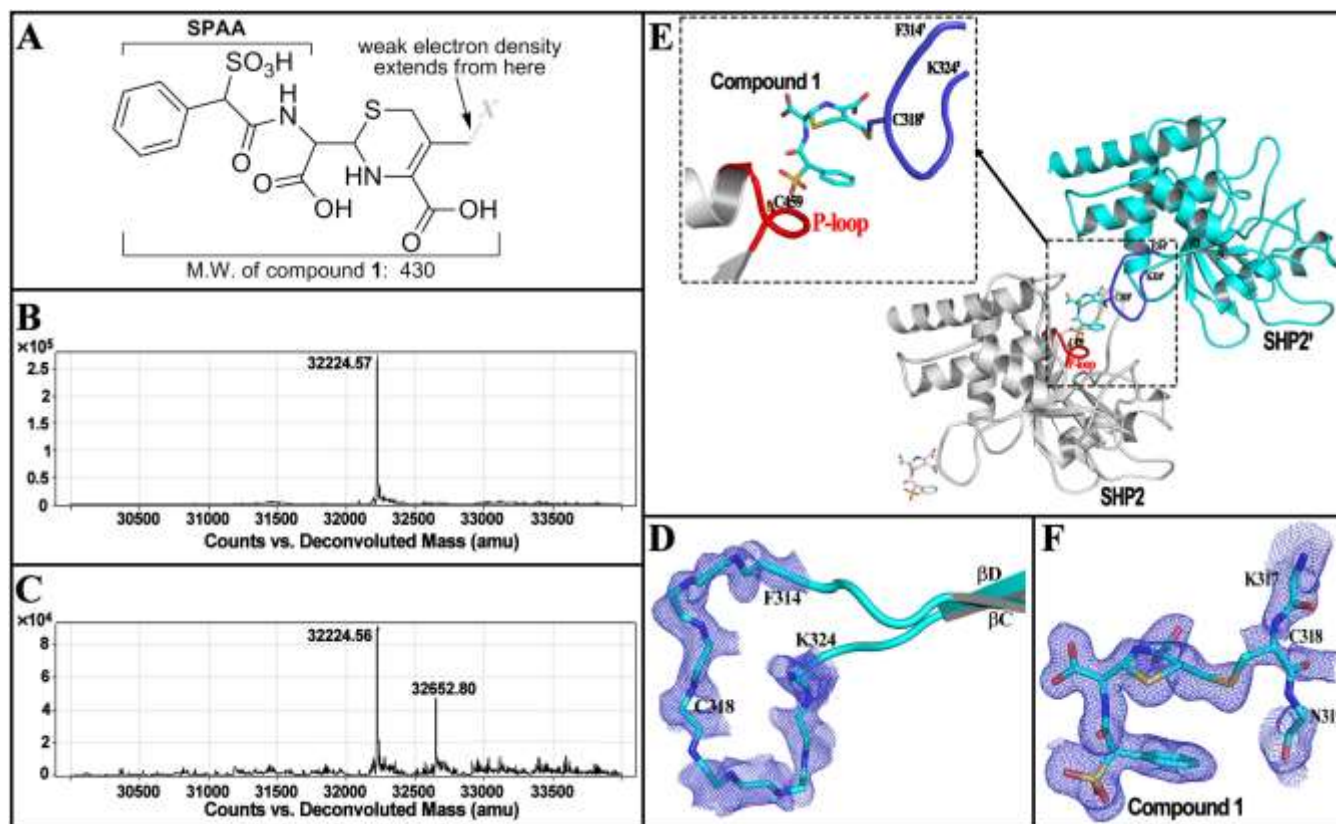


Figure S4. Compound 1 is covalently bonded with SHP2 under crystallization state. **A**): The chemical structure of unambiguously observed compound 1 in the co-crystal structure, and a highlight of the position from where continuous weak electron density extends. **B**): The QTOF ESI-MS data of re-dissolved SHP2 crystals shows a single peak at 32224.57. **C**): The QTOF ESI-MS data of re-dissolved co-crystal of SHP2 with cefsulodin shows the protein peak at 32224.56 and an additional peak at 32652.80, and the difference of 428.24 corresponds to a molecular mass of compound 1 after covalent bonding with SHP2. **D**): The 2Fo-Fc electron density map (contoured at 1.0 σ) around the backbone atoms (C, Ca and N, shown in stick) of the flexible loop (residues 314-324). **E**): Compound 1, binding at SHP2 active site, is covalently bonded to C318 from a nearby symmetric SHP2 molecule. **F**): The 2Fo-Fc electron density map (contoured at 0.7 σ) around the compound 1 indicates the covalent bond formation.

8. Figure S5

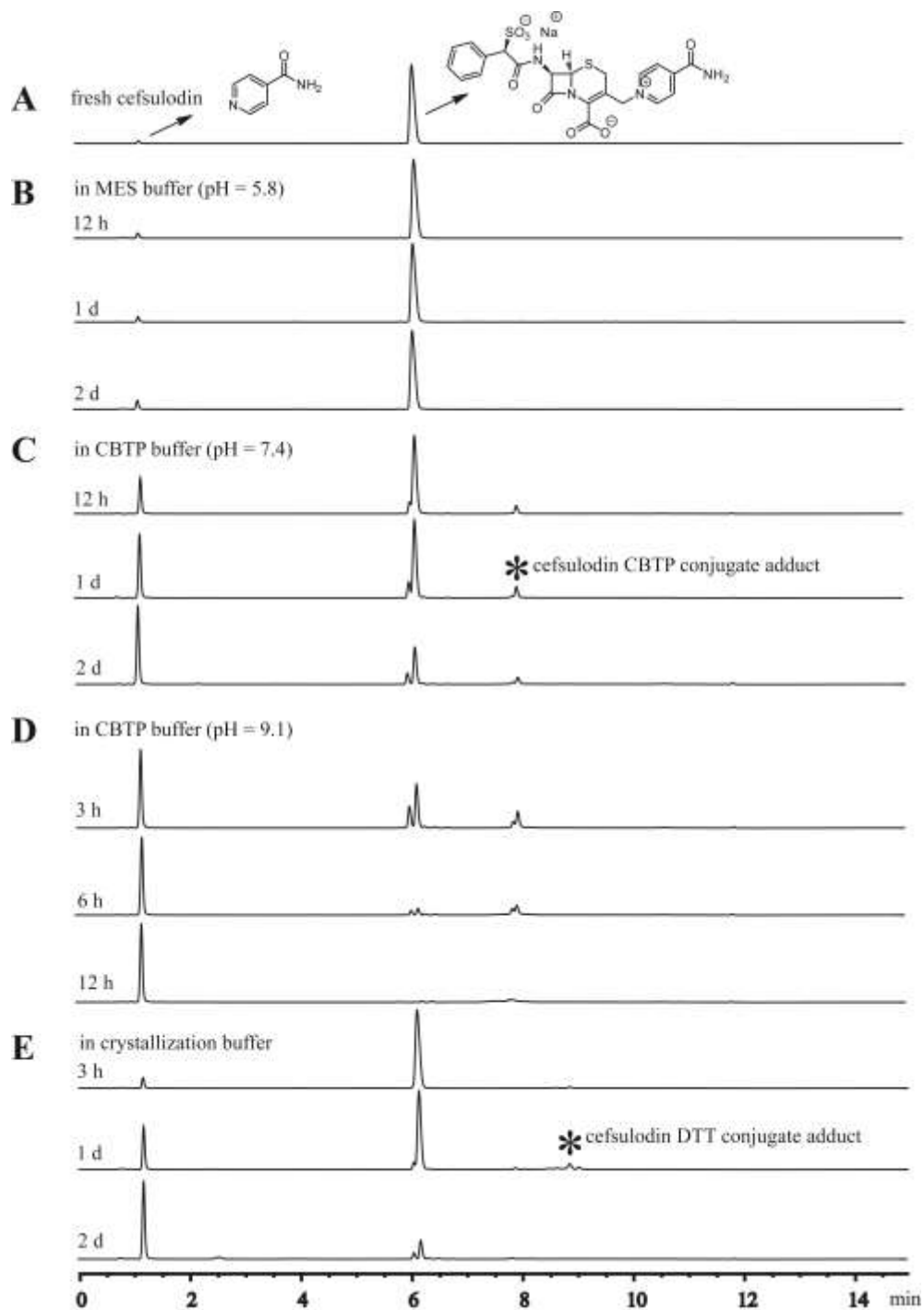


Figure S5. Stability of cefsulodin under various conditions. **A)** LC-MS analysis of freshly prepared cefsulodin in pH 7.0 buffer containing 50 mM 3,3-dimethylglutarate and 1 mM EDTA with an ionic strength of 0.15 M adjusted by addition of NaCl shows cefsulodin (retention time 6.1 min) is very pure with tiny amount of nicotinamide (retention time 1.0 min). **B)** In MES buffer with pH=5.8, cefsulodin and isonicotinamide concentrations are almost unchanged at all time points of 12 h, 1 d, 2 d, indicating cefsulodin is stable for at least 2 days. **C)** In CBTP buffer with pH=7.4, cefsulodin concentrations decreased progressively with the increase of isonicotinamide concentration through time points of 12 h, 1 d,

2 d, the minor peak at retention time 7.9 min belongs to cefsulodin and CBTP conjugated product (see **Figure S6A**). Minor peak (retention time 6.0 min) left to cefsulodin belongs to racemized cefsulodin.³ **D**): In CBTP buffer with pH=9.1, cefsulodin concentrations decreased rapidly with the increase of isonicotinamide concentration through time point of 3 h, 6 h, 12 h, and cefsulodin was gone after 12 h. **E**): In crystallization solution, cefsulodin concentrations decreased progressively with the increase of isonicotinamide concentration through time points of 3 h, 1 d, 2 d, and the majority of cefsulodin was gone after 2 d, the minor peak at retention time 8.8 min belongs to cefsulodin and DTT conjugated product (see **Figure S6B**).

9. Figure S6

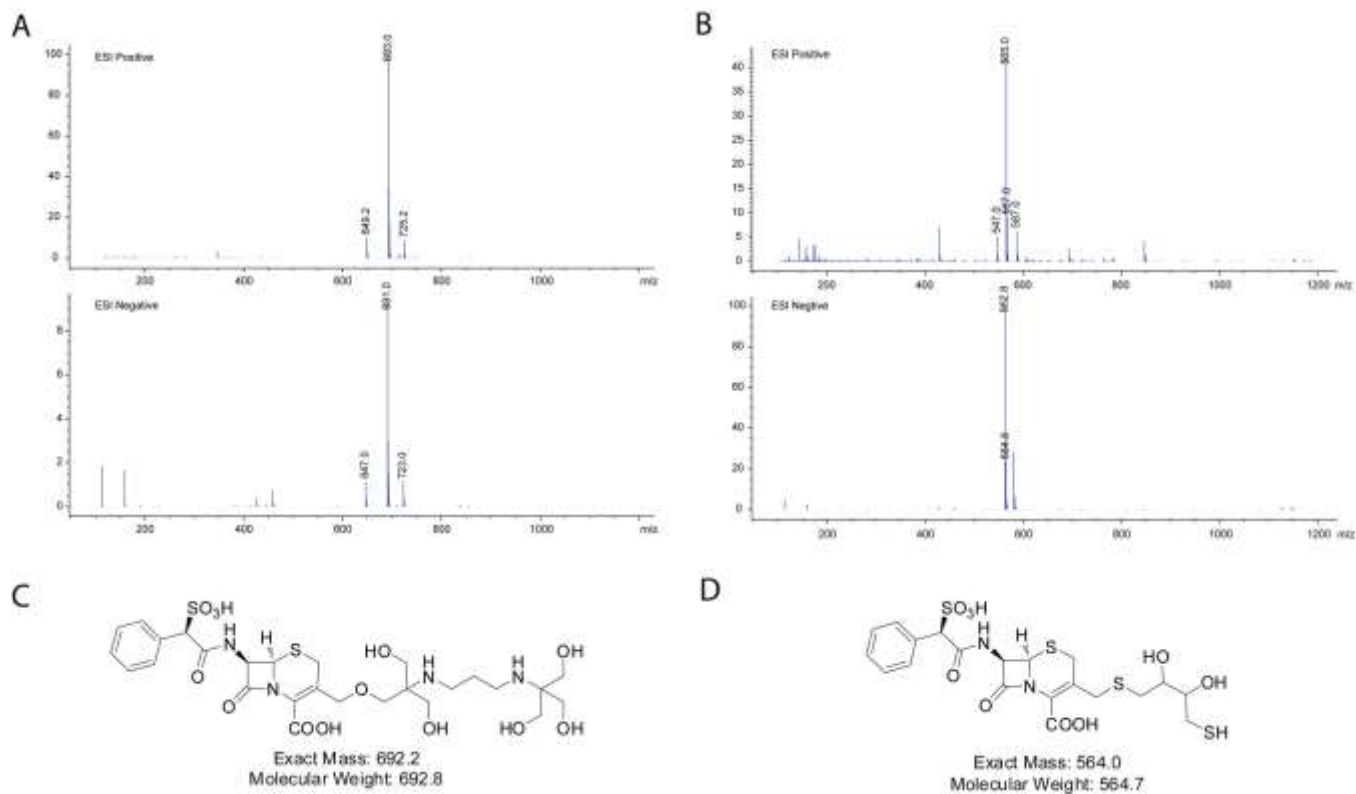


Figure S6. ESI-MS data of cefsulodin and buffer components. **A)** ESI-MS data of the minor peak at retention time 7.9 min in **Figure S5C** middle spectrum shows the positive ion at 693.0 and the negative ion at 691.0, indicating the existence of a molecule with mass around 692.0. **B)** ESI-MS data of the minor peak at retention time 8.8 min in **Figure S5E** middle spectrum shows the positive ion at 565.0 and the negative ion at 563.0, indicating the existence of a molecule with mass around 564.0. **C)** The chemical structure, exact mass, and molecule weight of a conjugate adduct of cefsulodin and CBTP, corresponding to the molecule with a retention time of 7.9 min in **Figure S5C** middle spectrum. **D)** The chemical structure, exact mass, and molecule weight of a conjugate adduct of cefsulodin and DTT, corresponding to the molecule with a retention time of 8.8 min in **Figure S5E** middle spectrum.

10. Figure S7

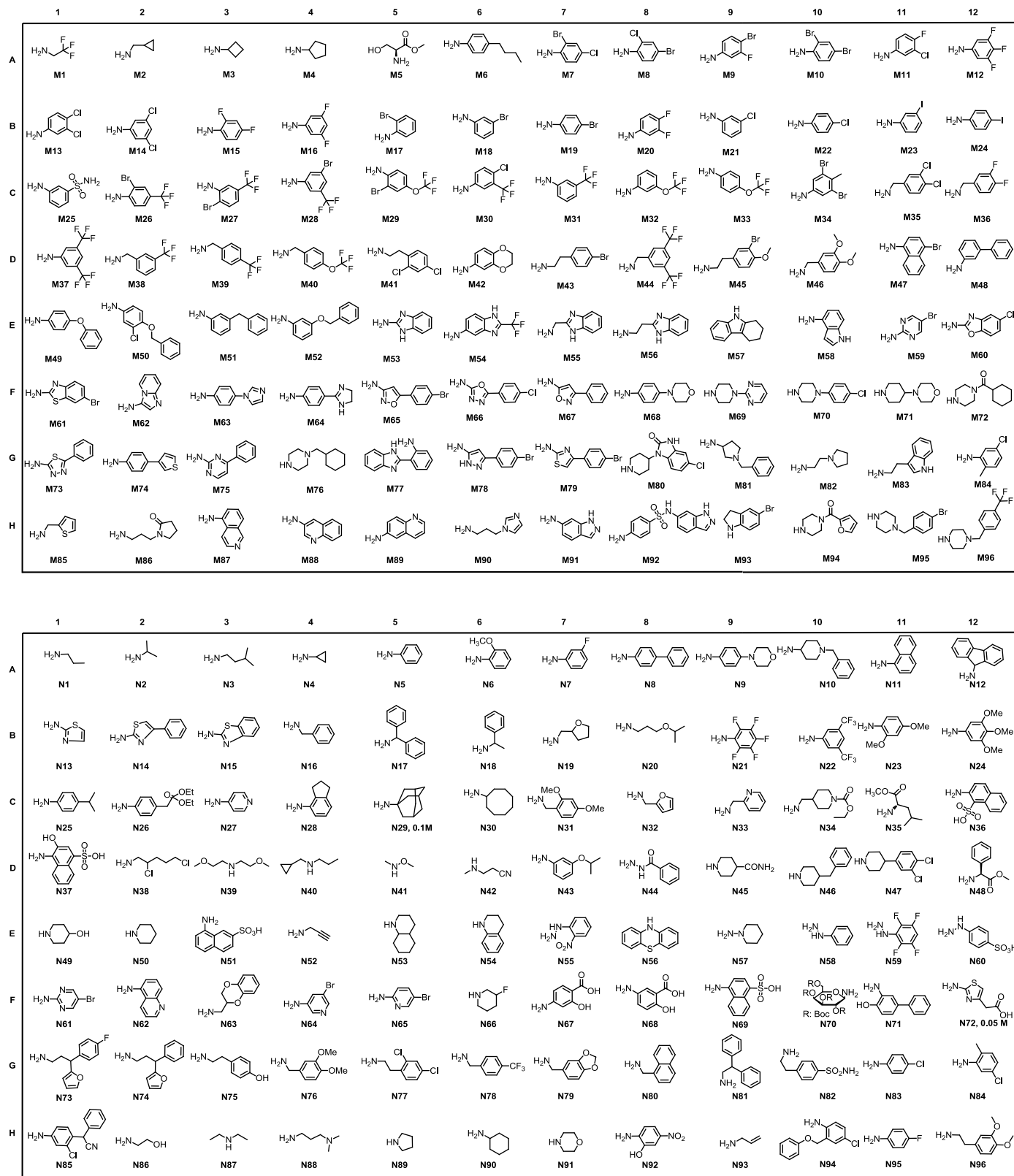
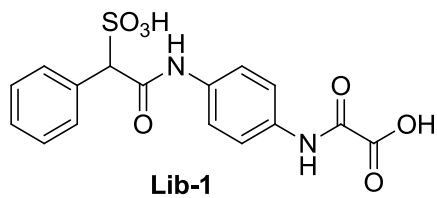
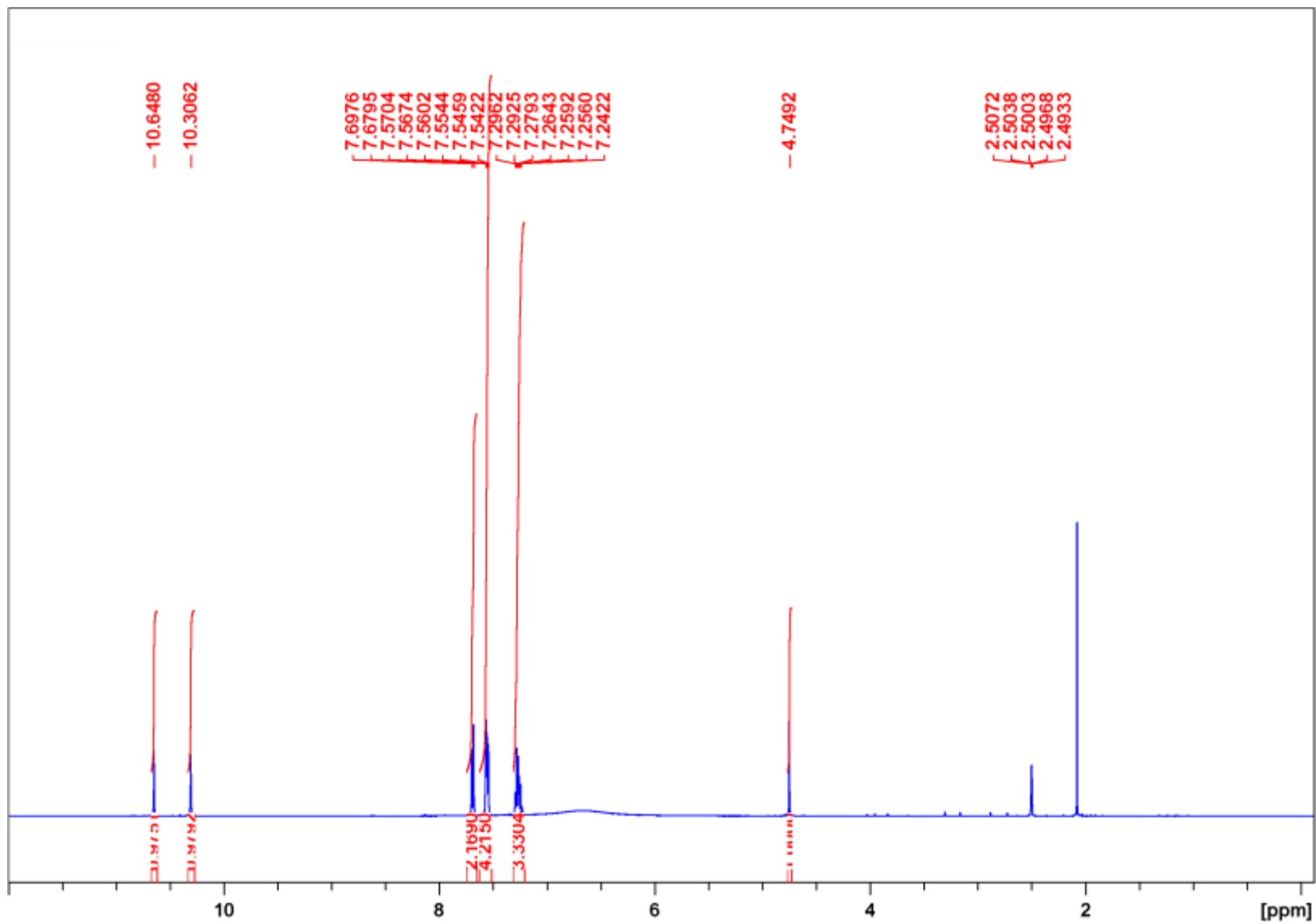
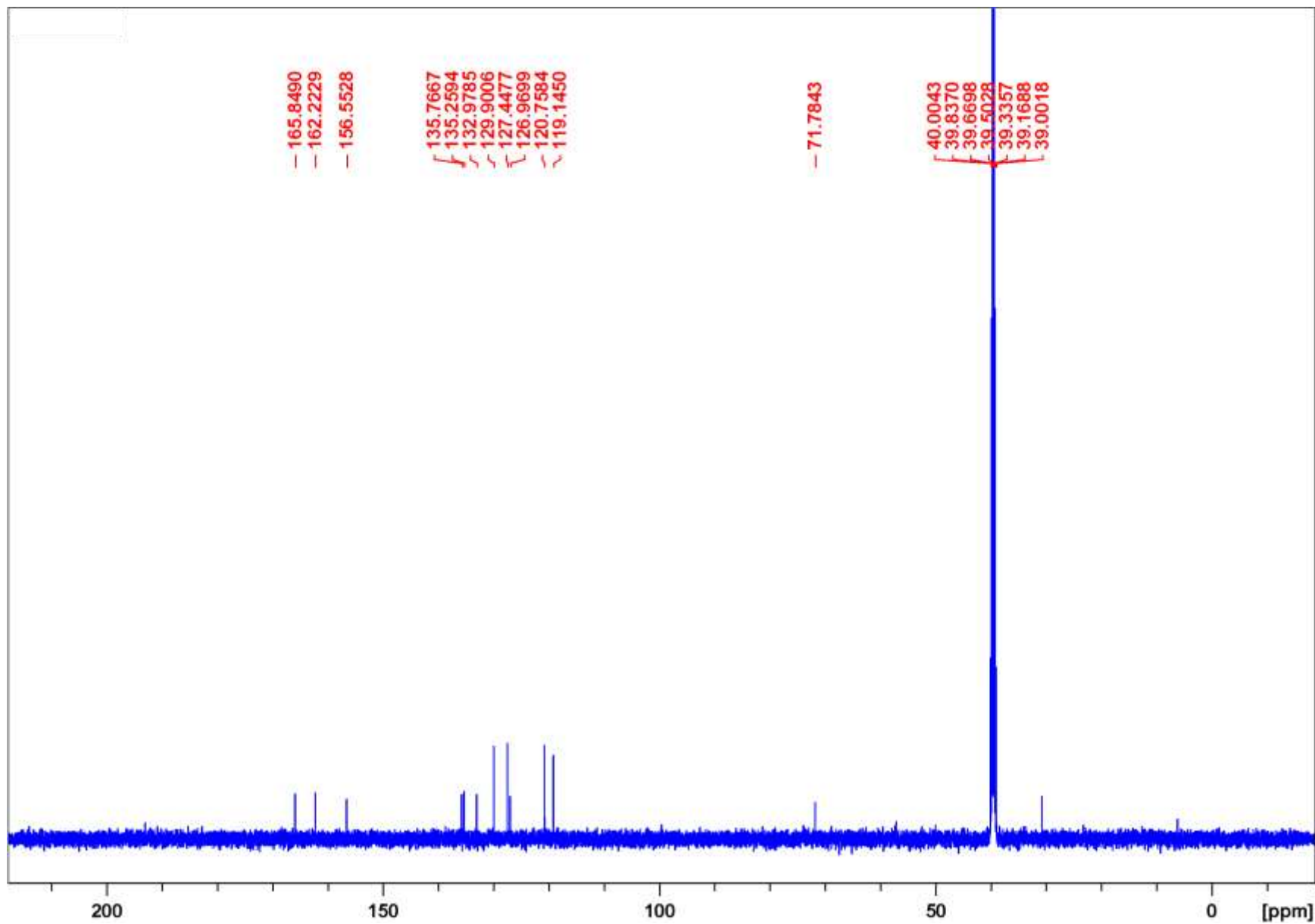


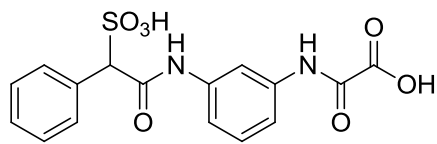
Figure S7. Chemical structures of a set of 192 amines.

11. NMR spectra of Lib-1 to Lib-4, and compounds 2 to 5

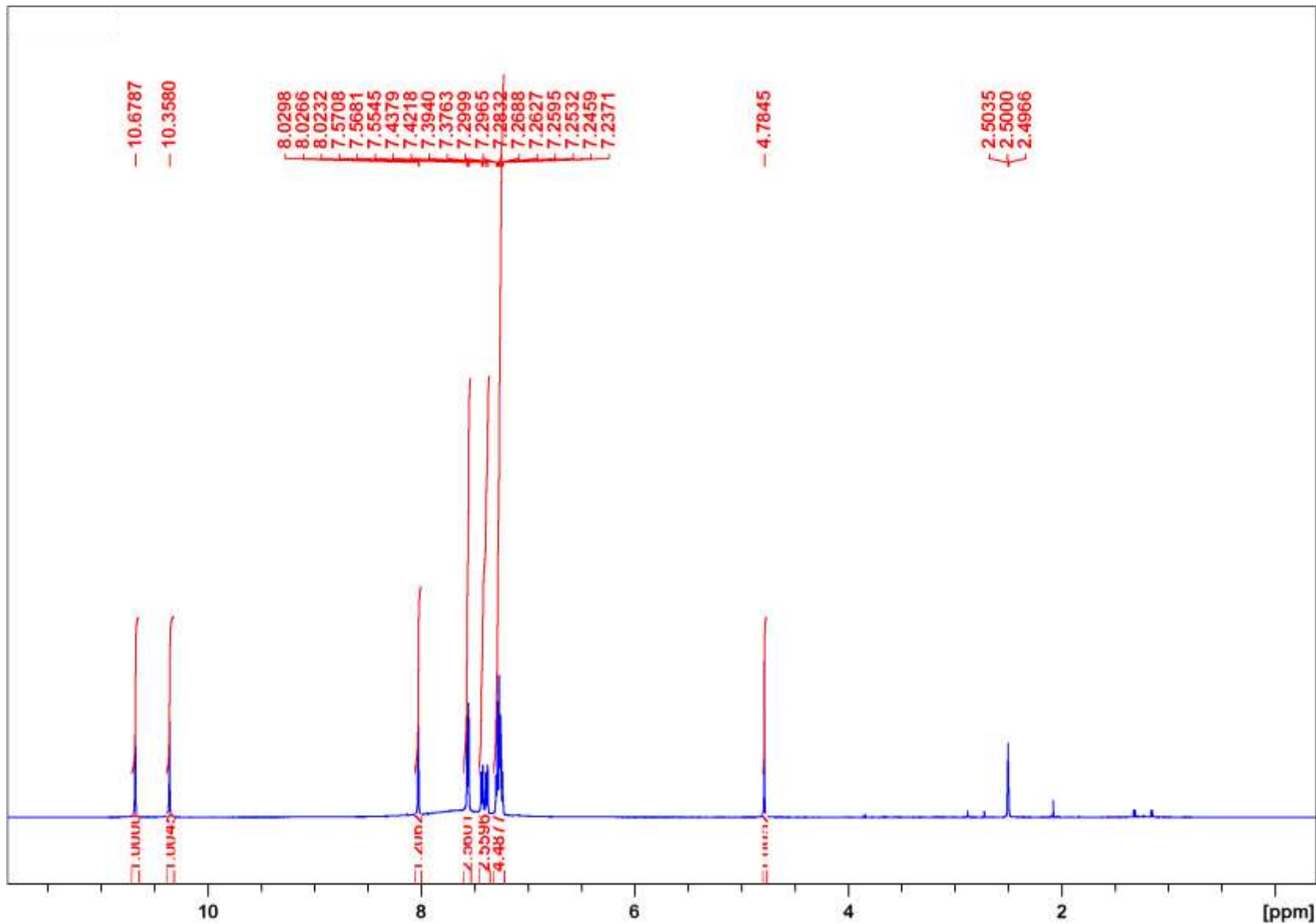


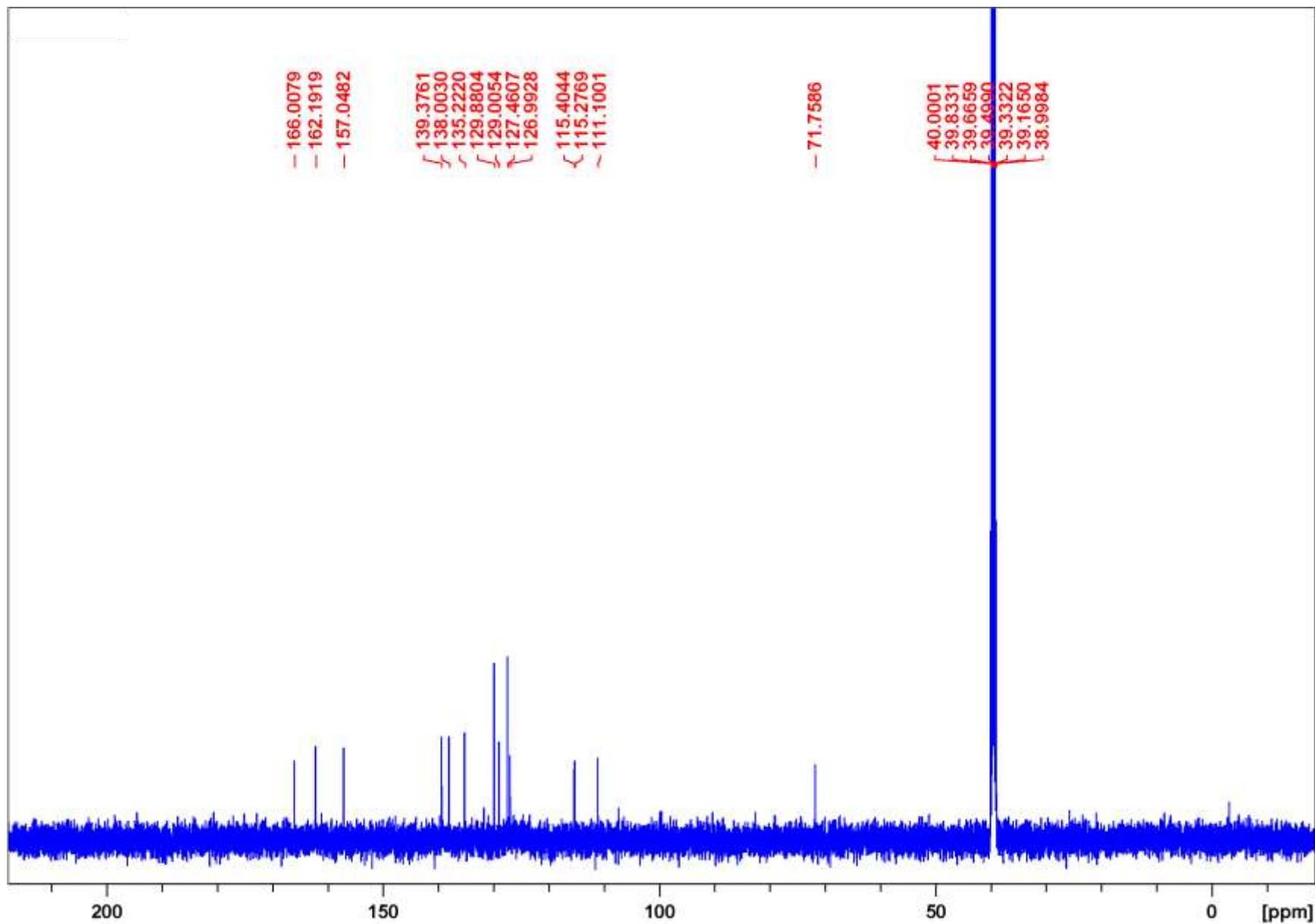


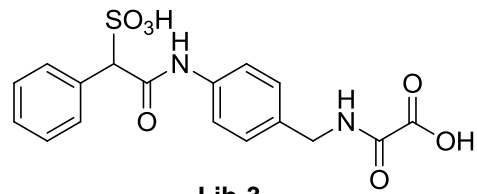




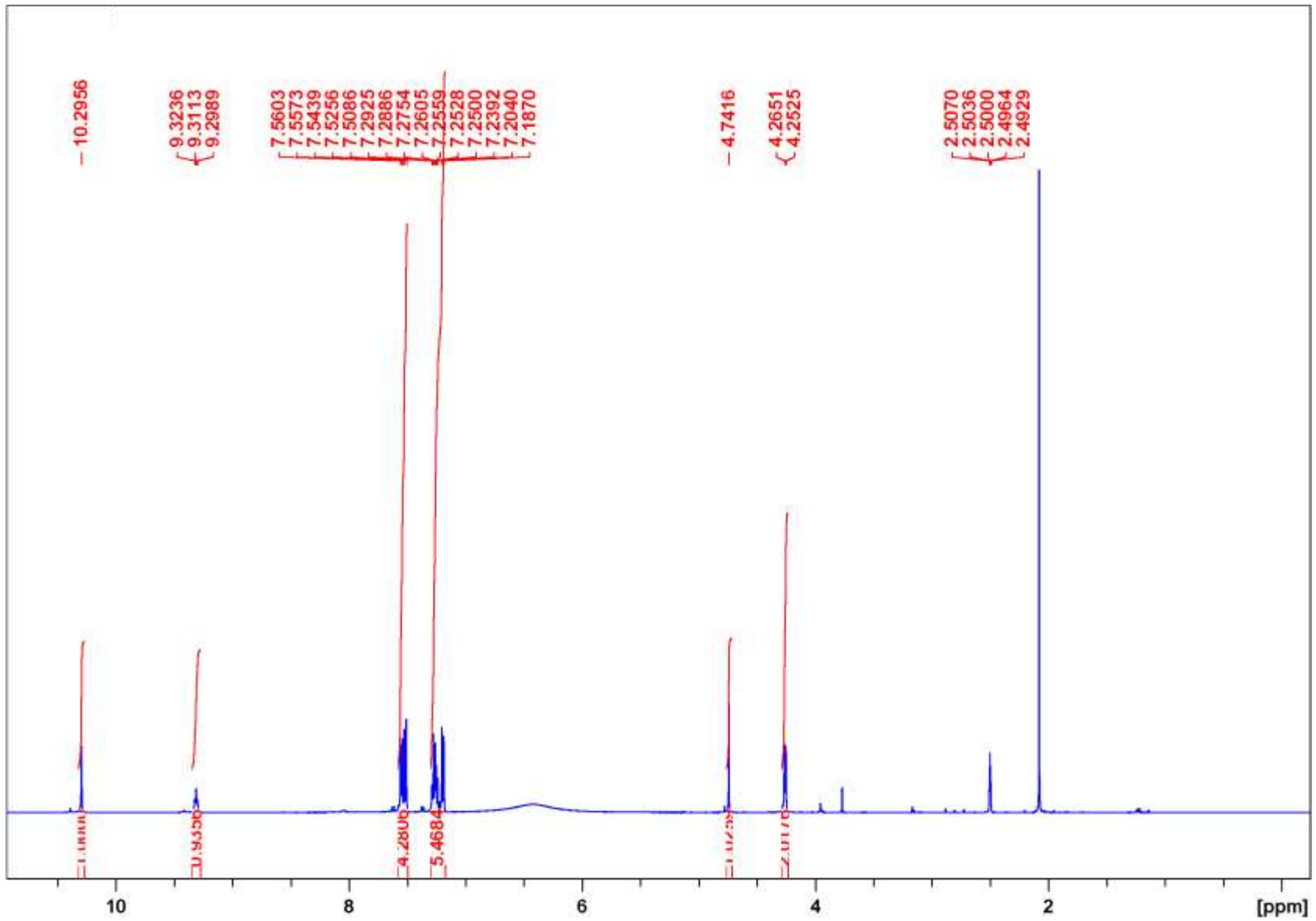
Lib-2

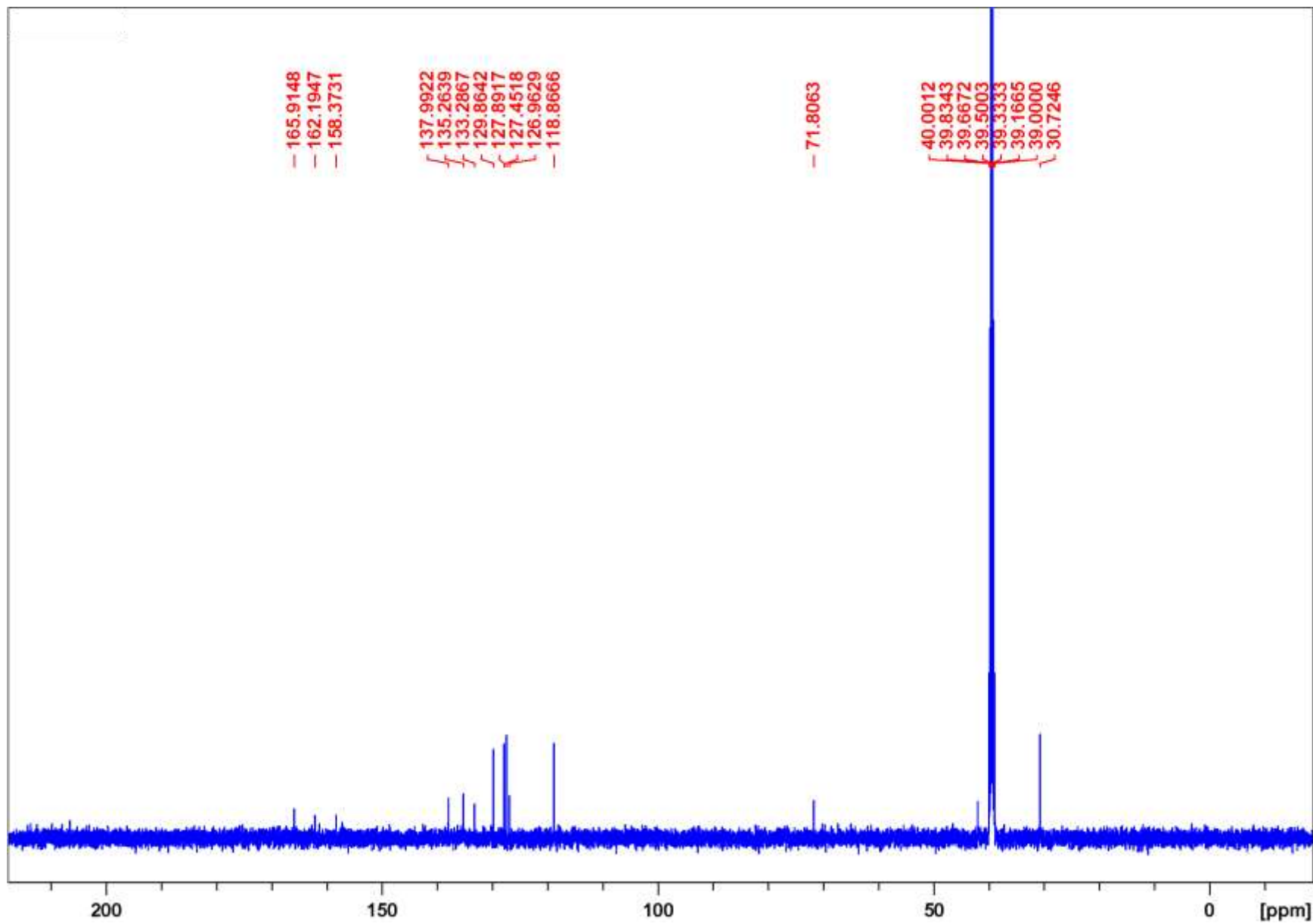


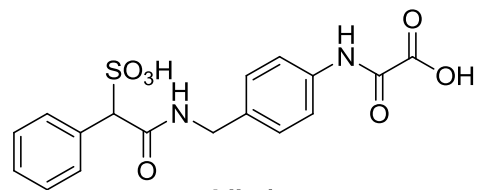




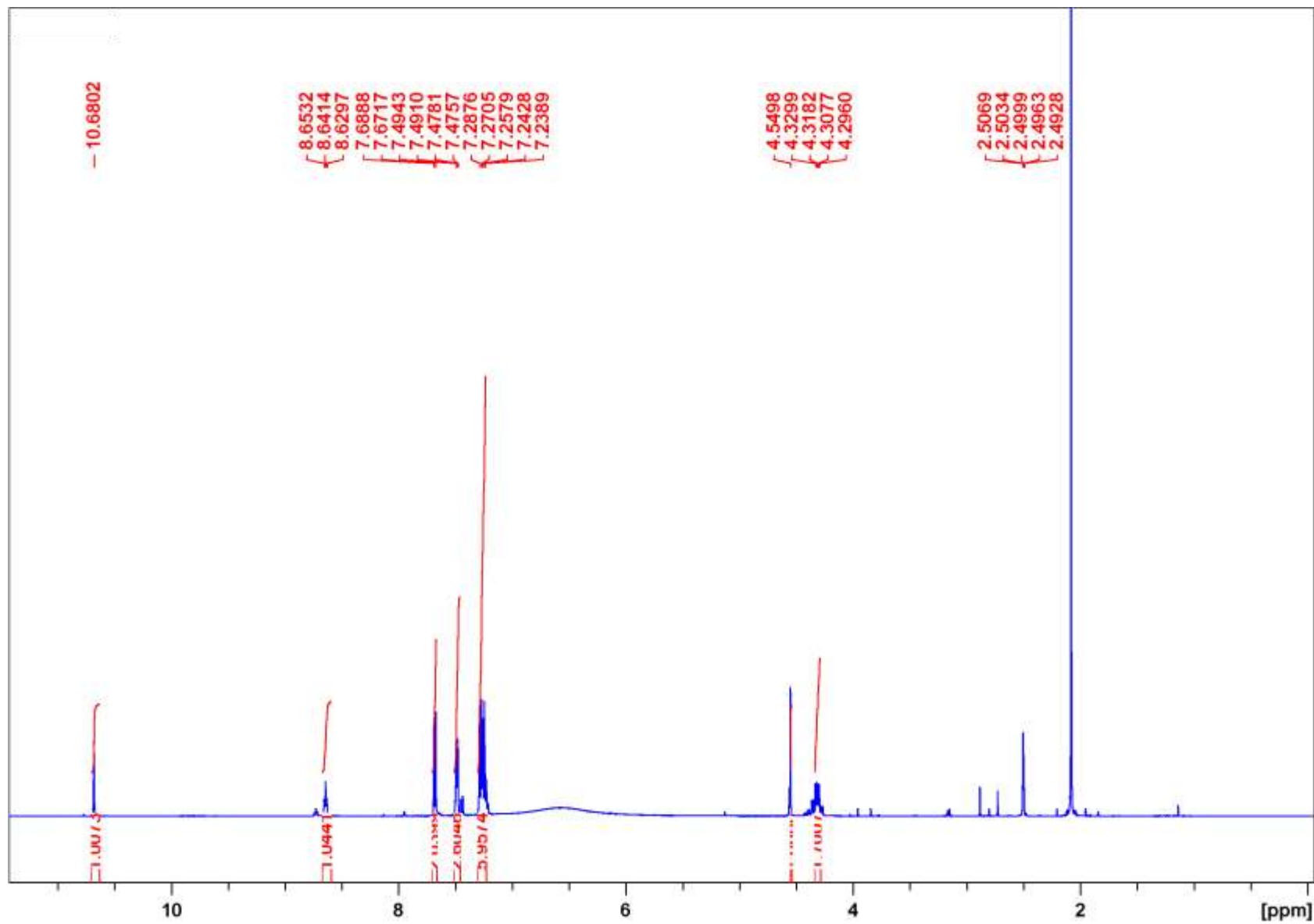
Lib-3

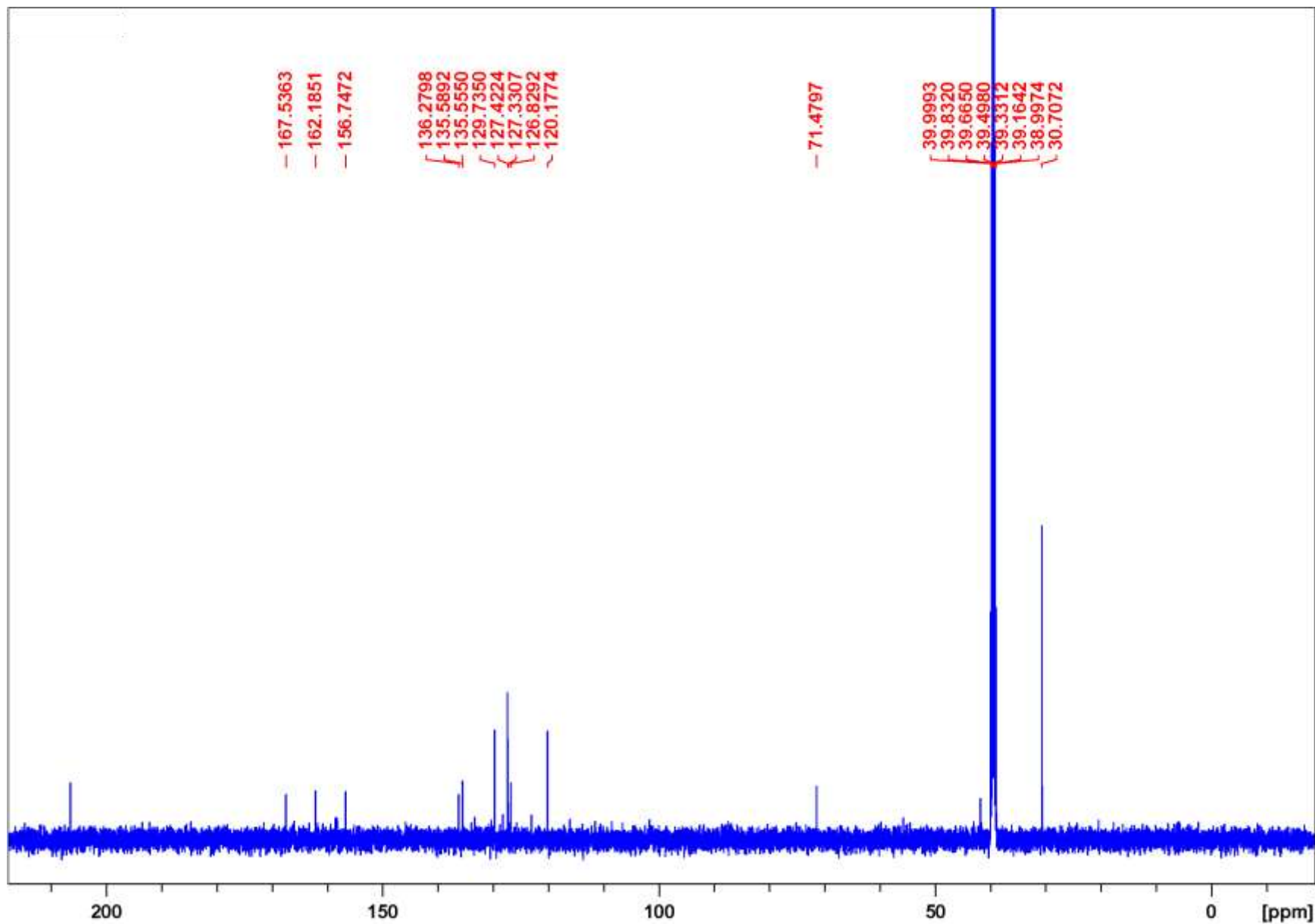


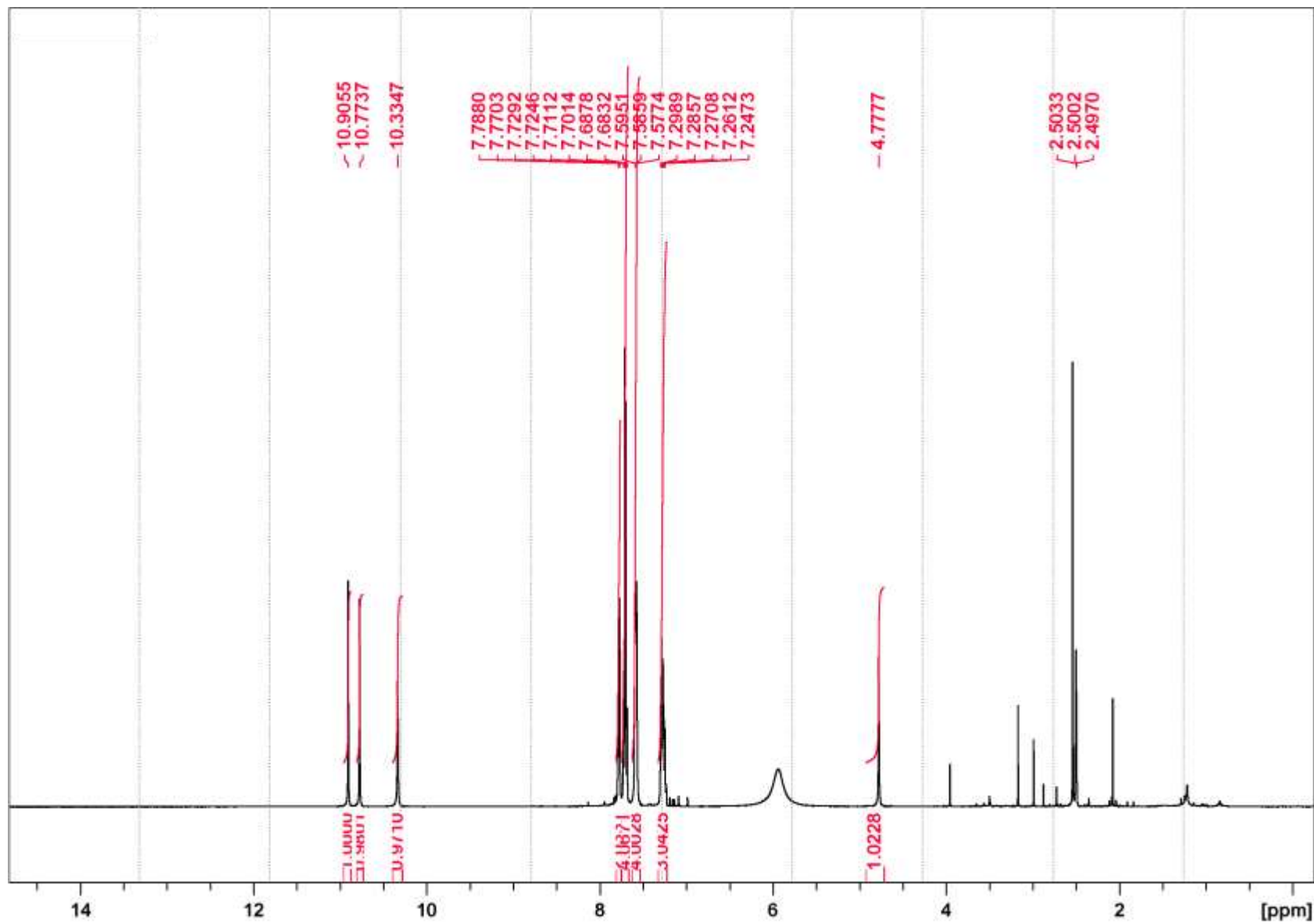
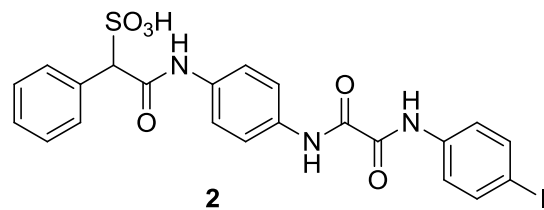


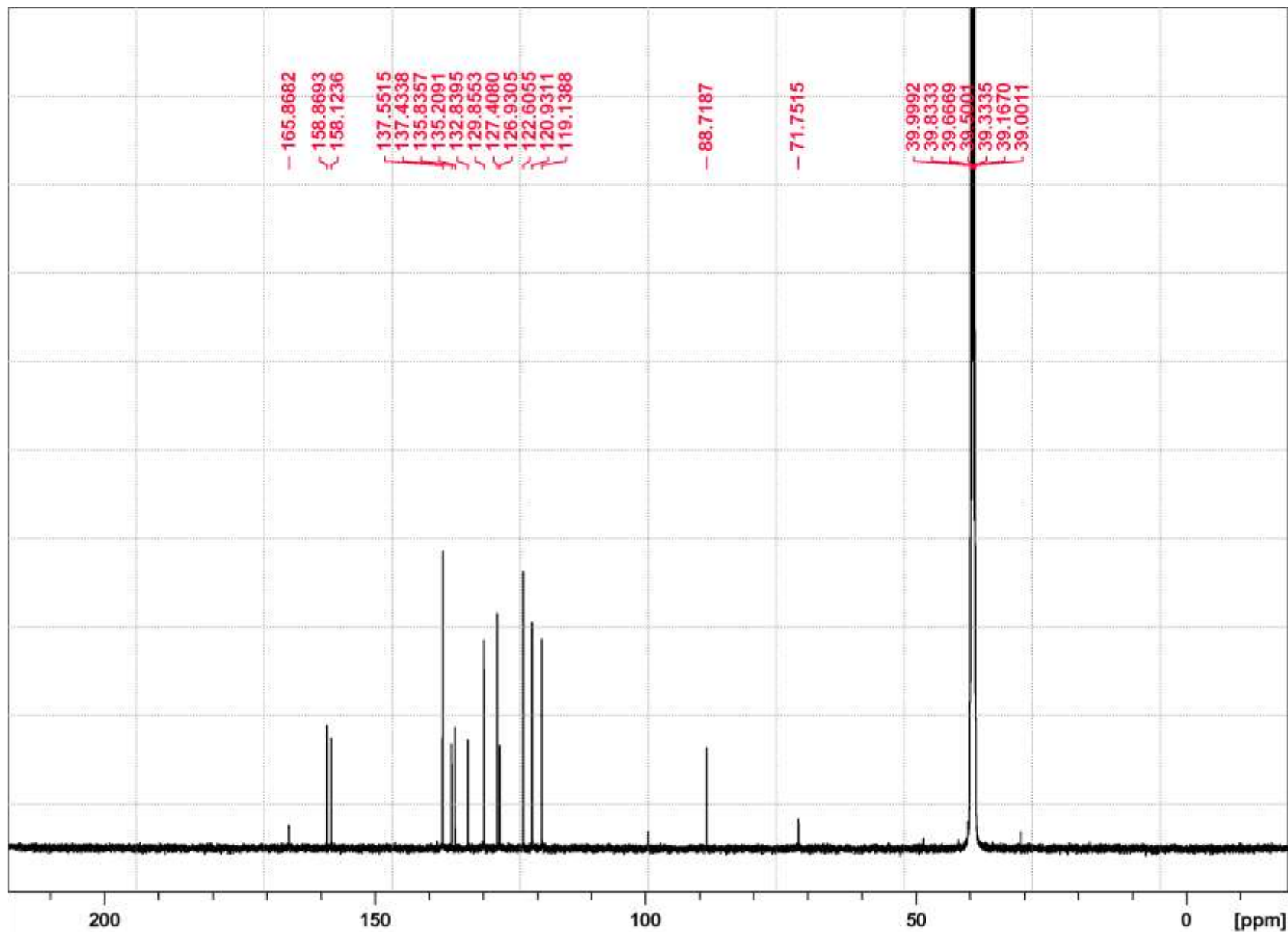


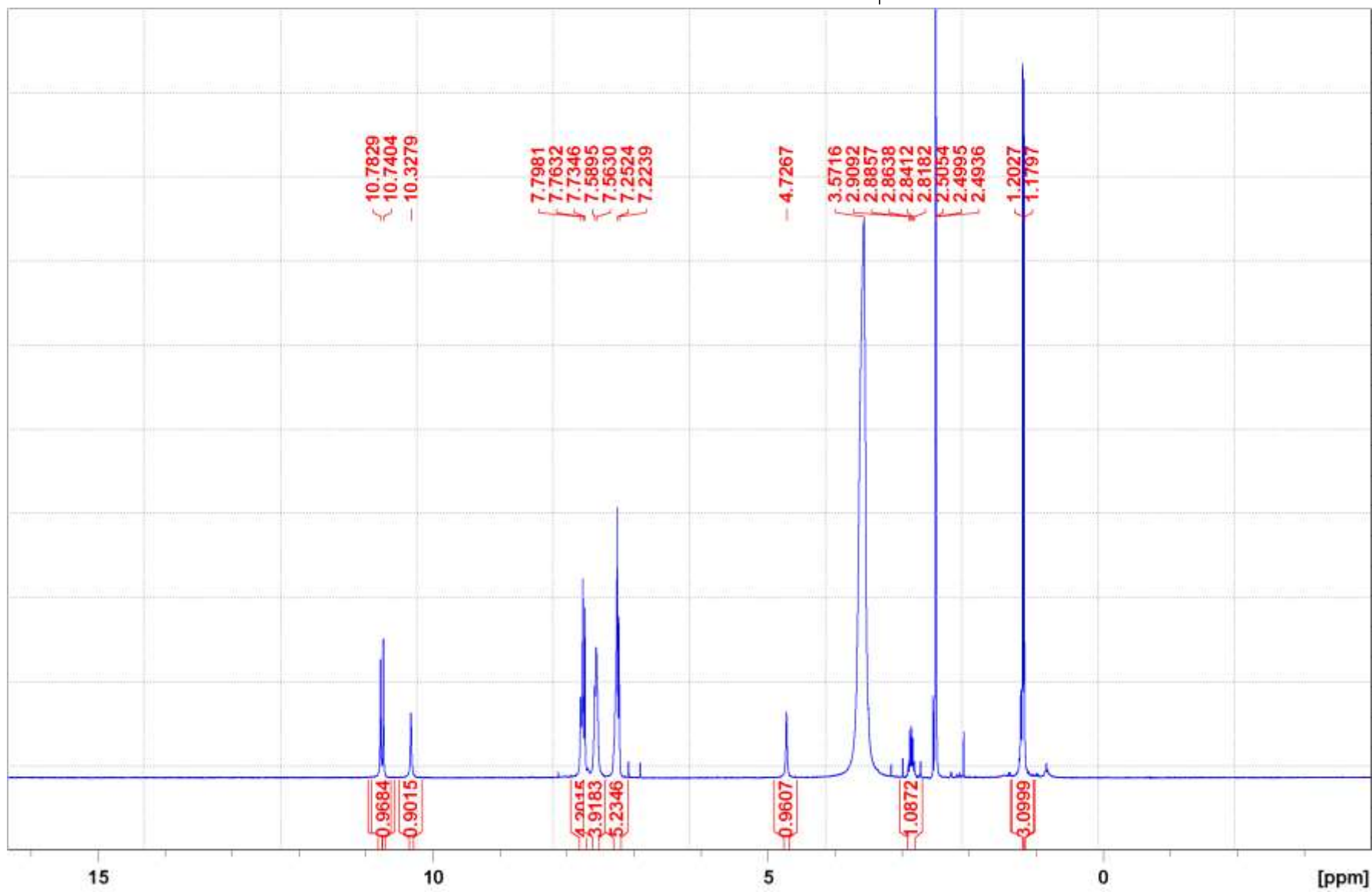
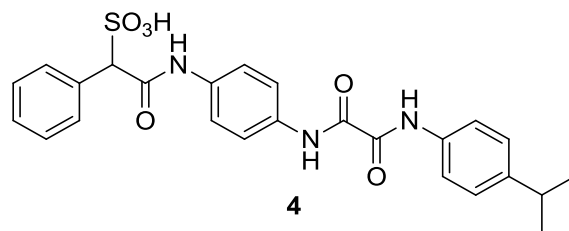
Lib-4

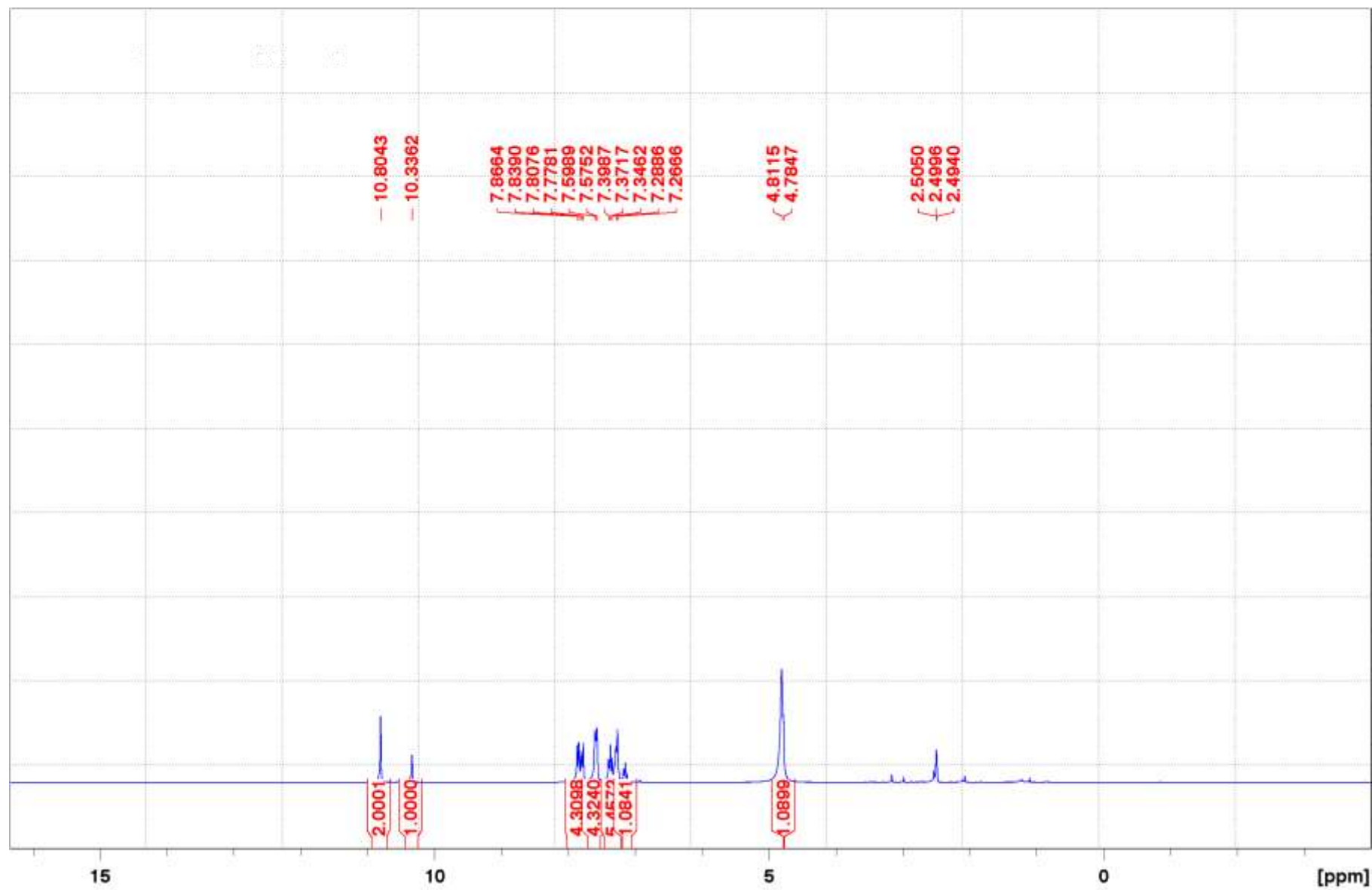
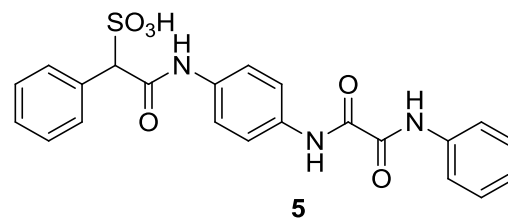


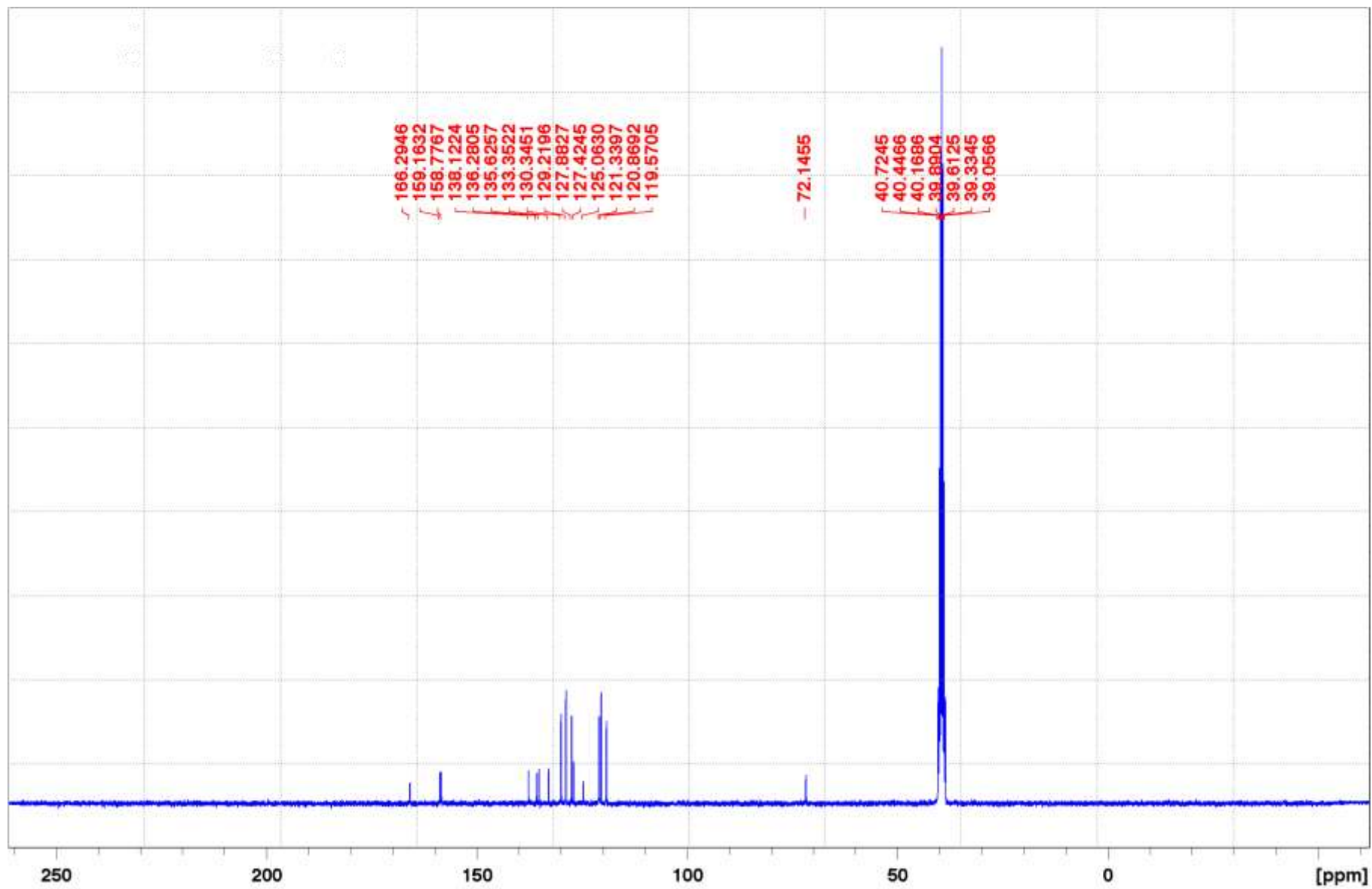




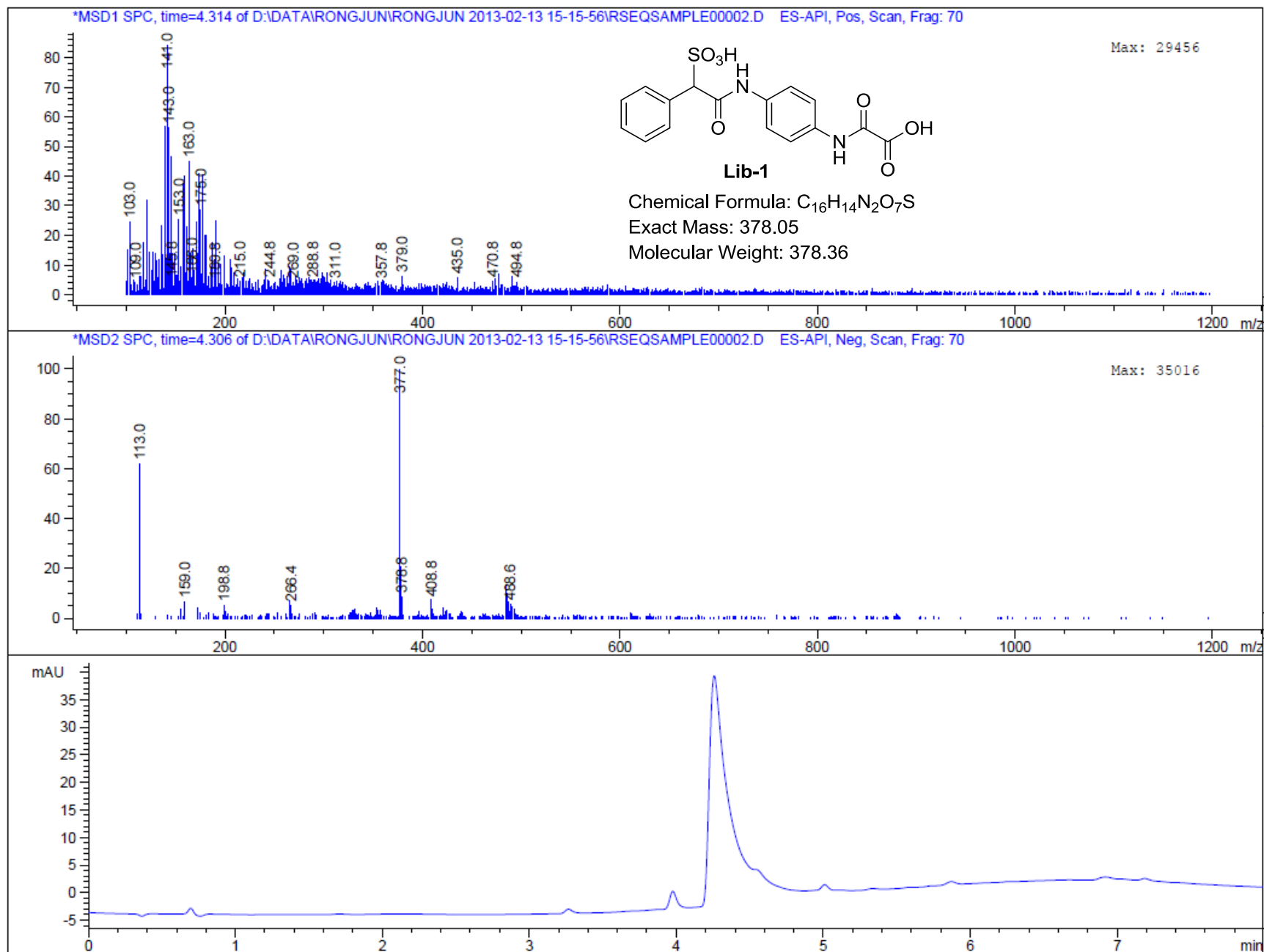


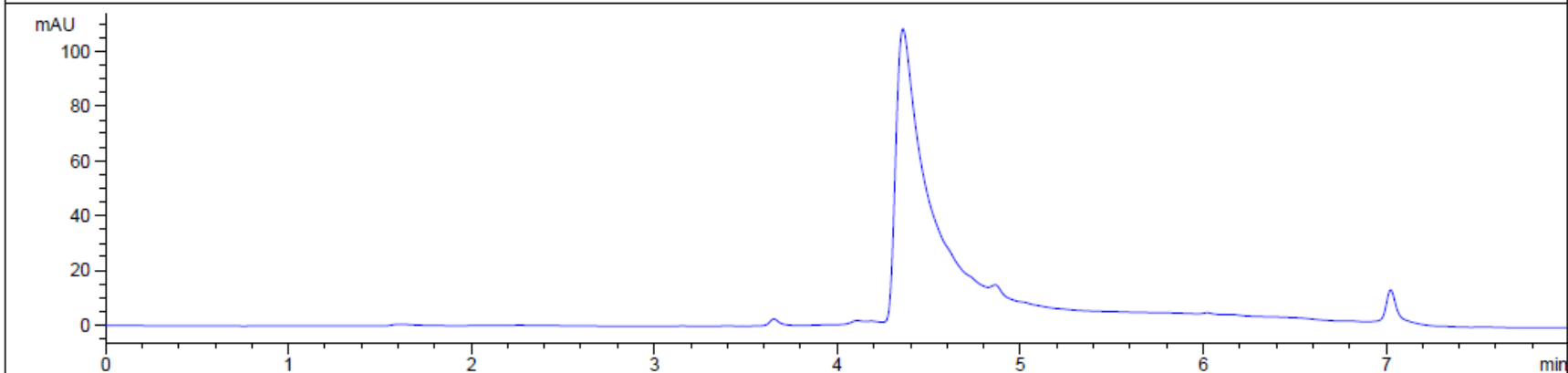
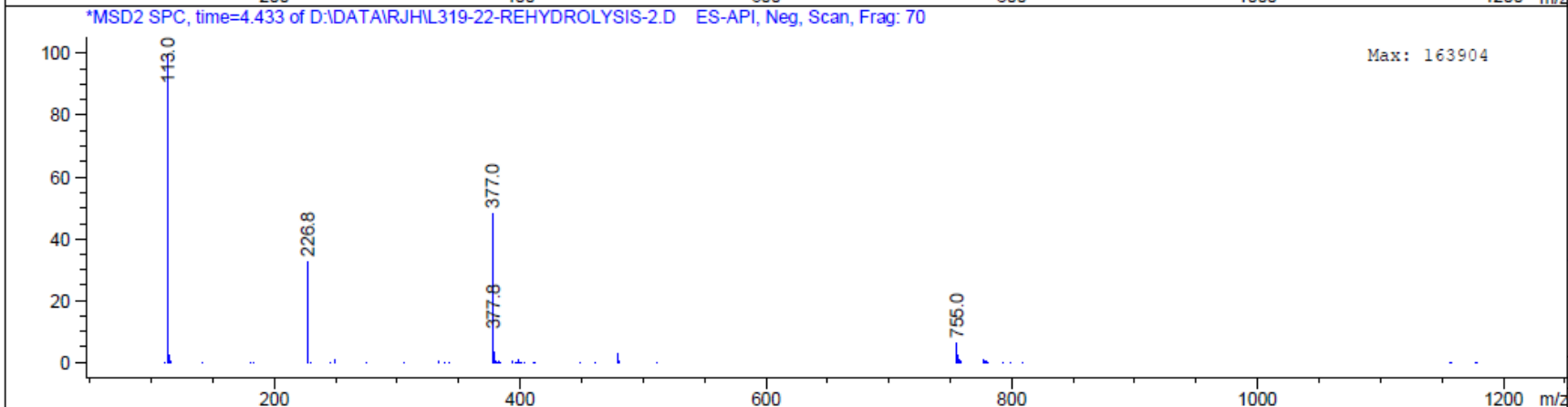
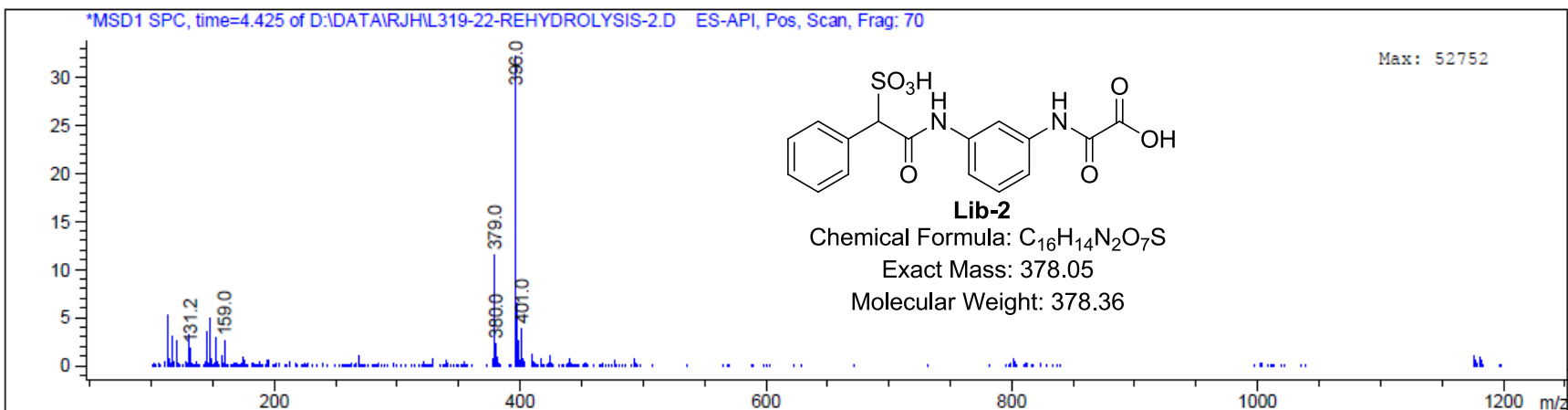


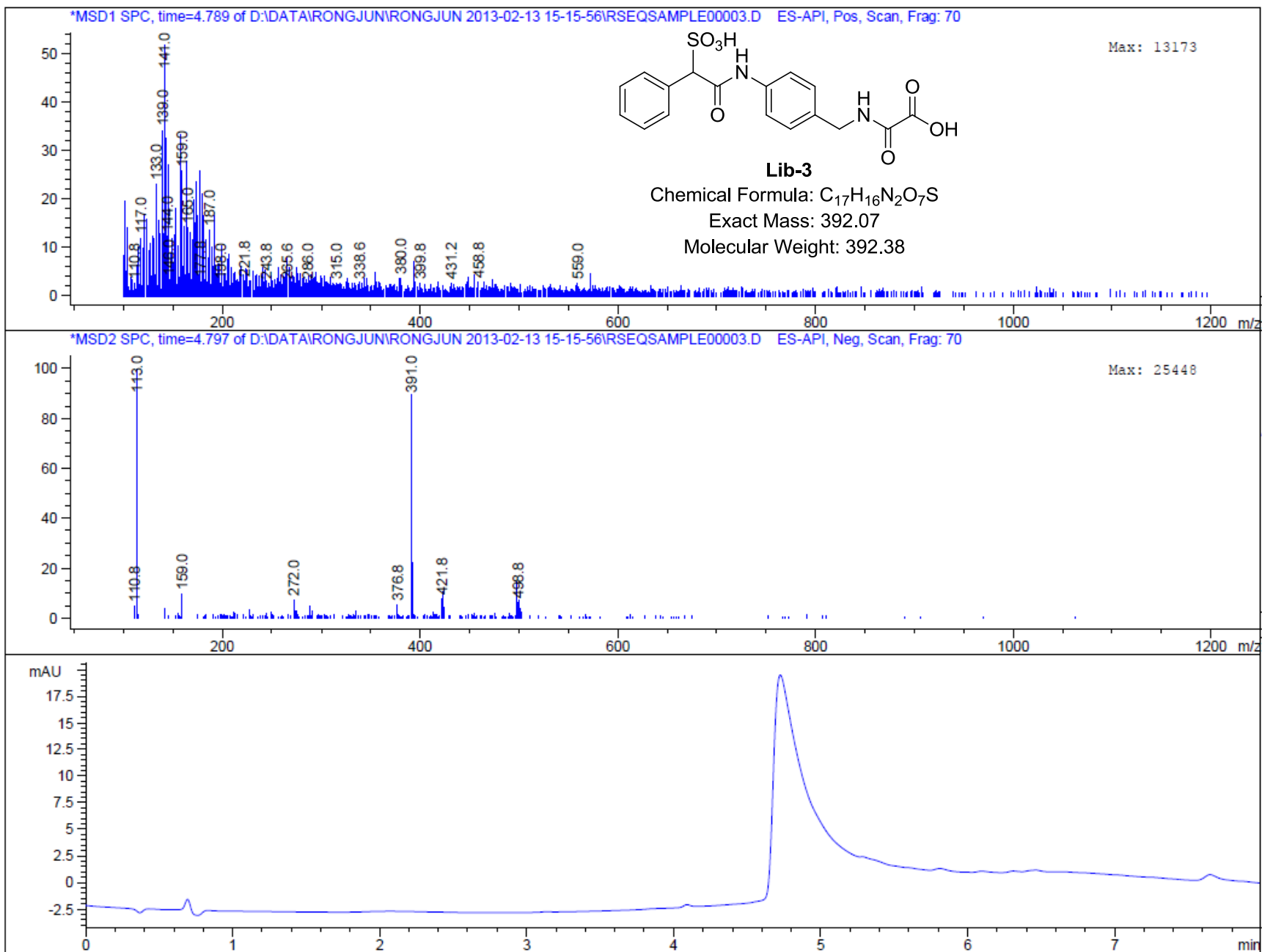


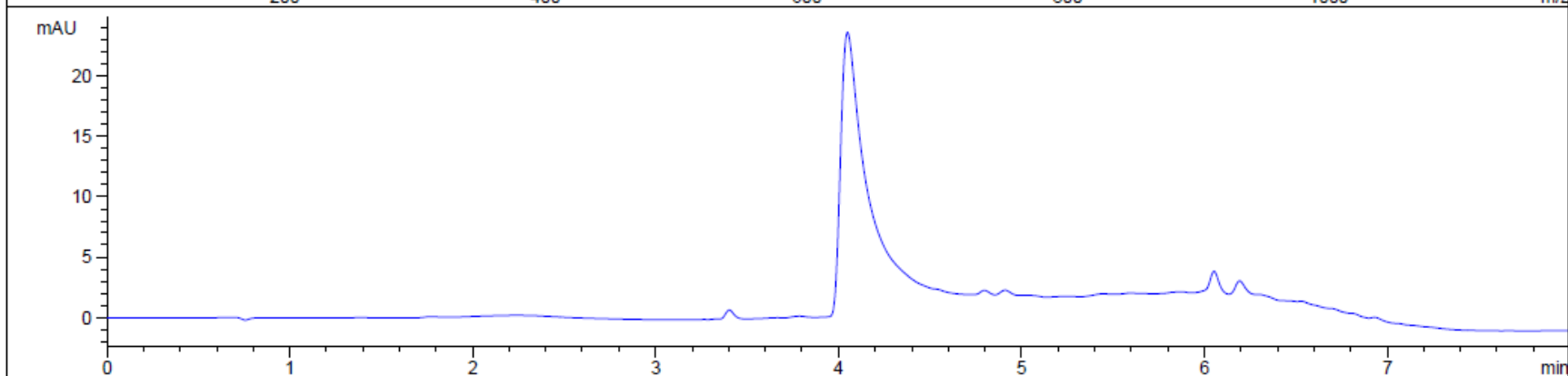
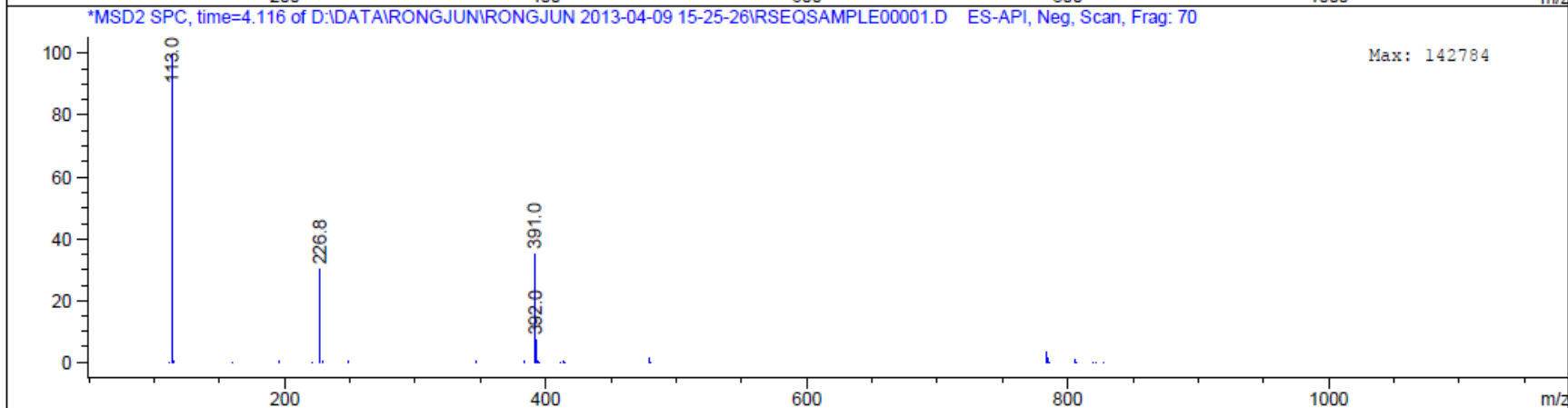
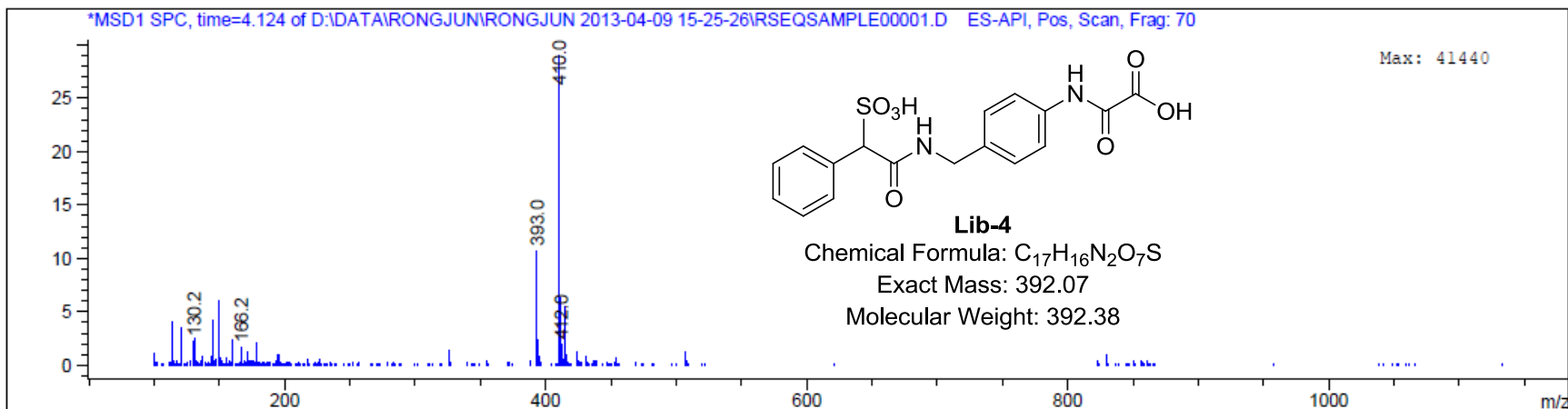


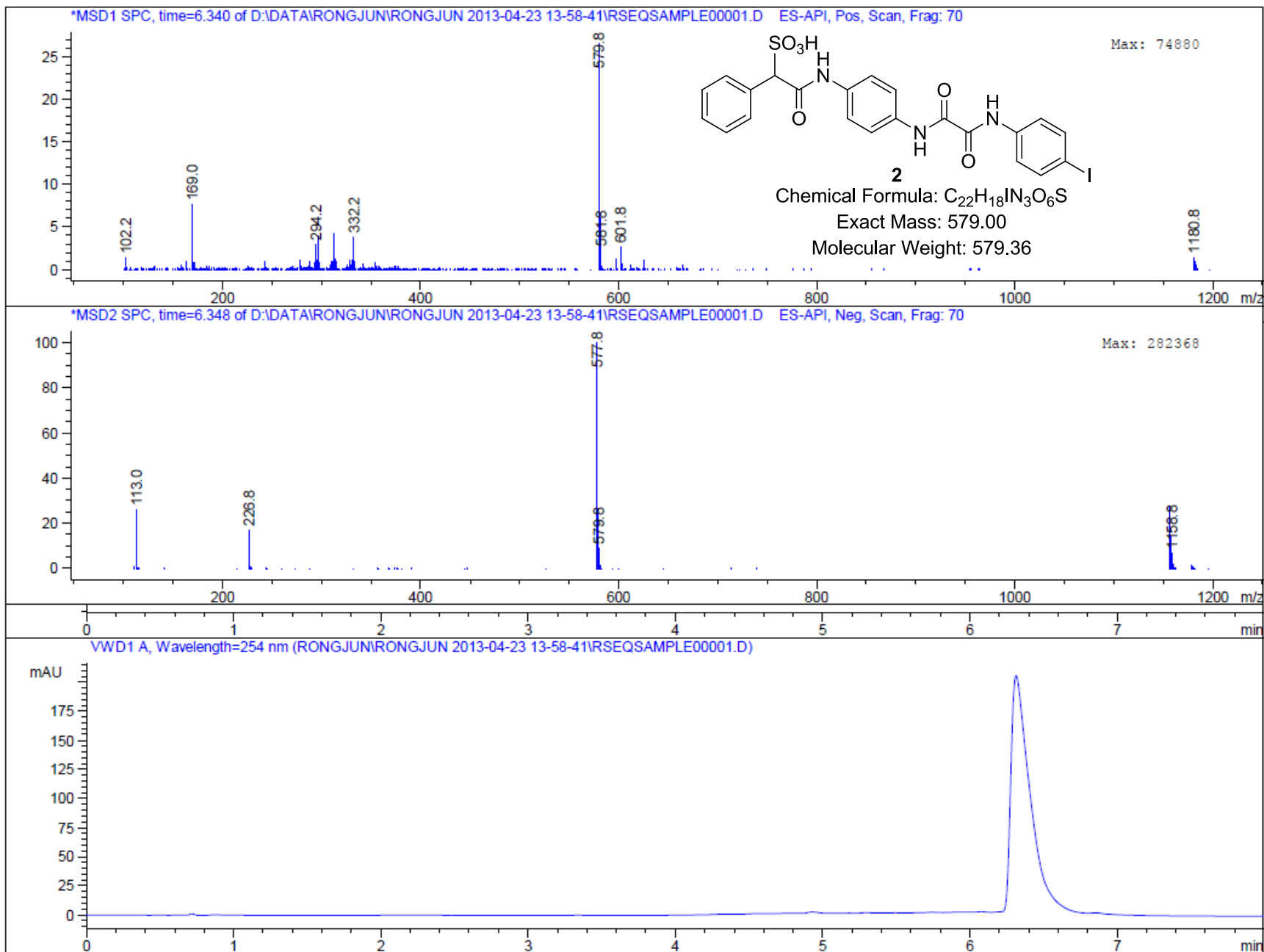
12. LC-MS spectra of Lib-1 to Lib-4, and compounds 2 to 5



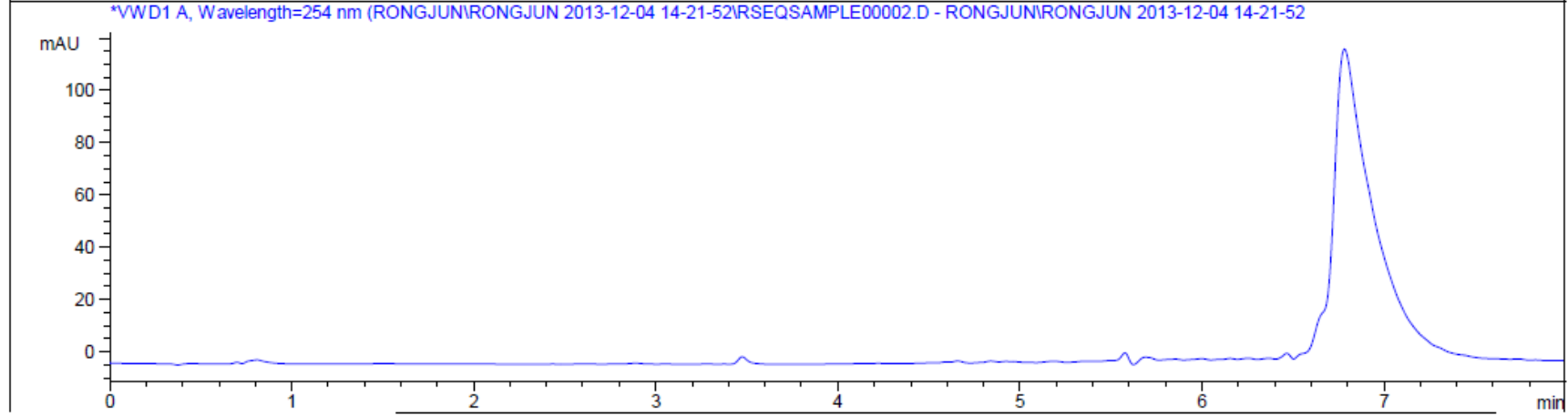
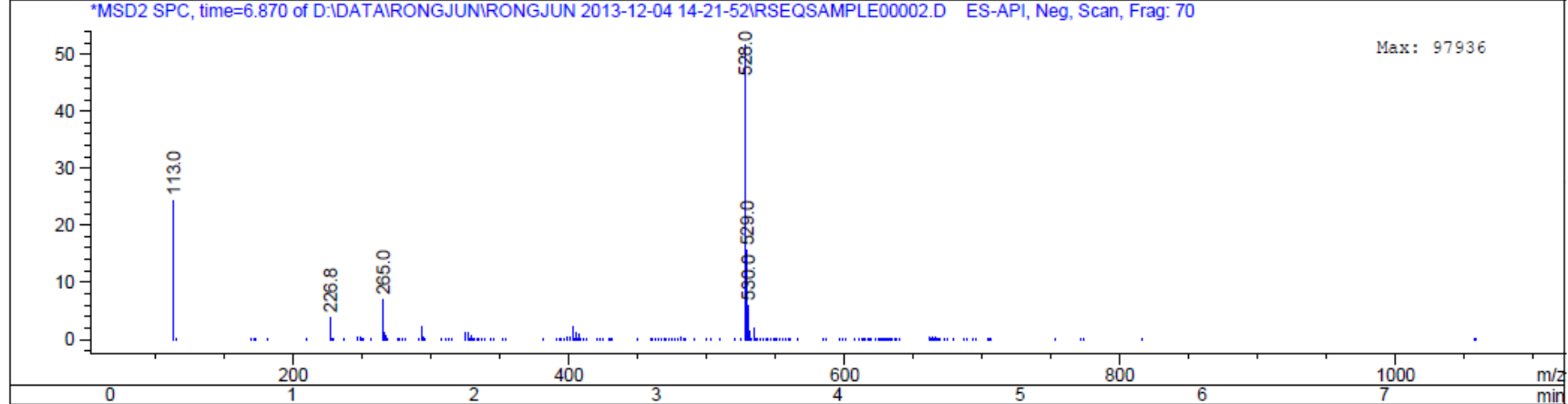
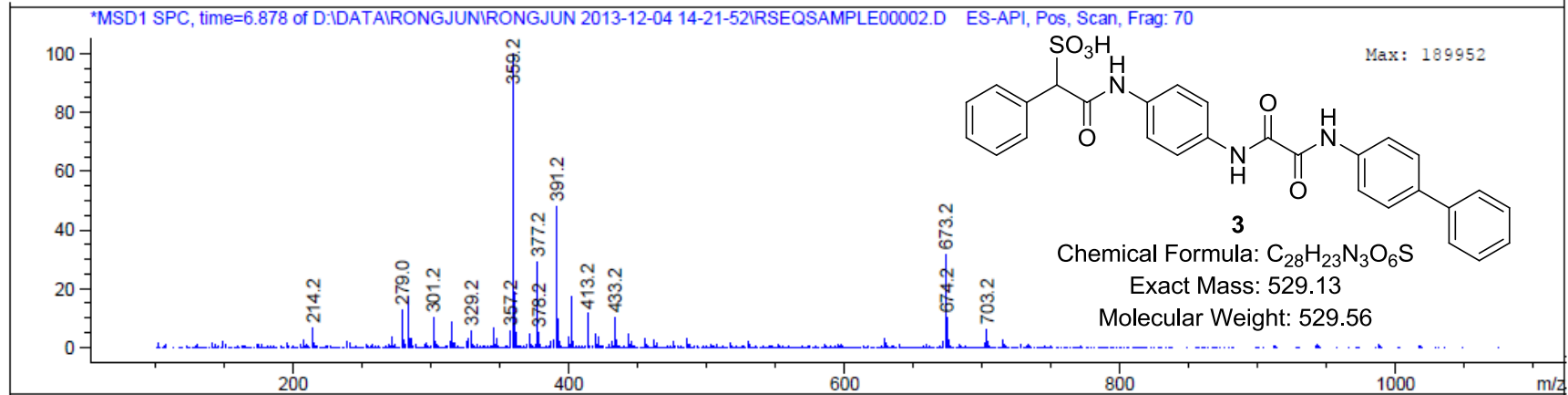




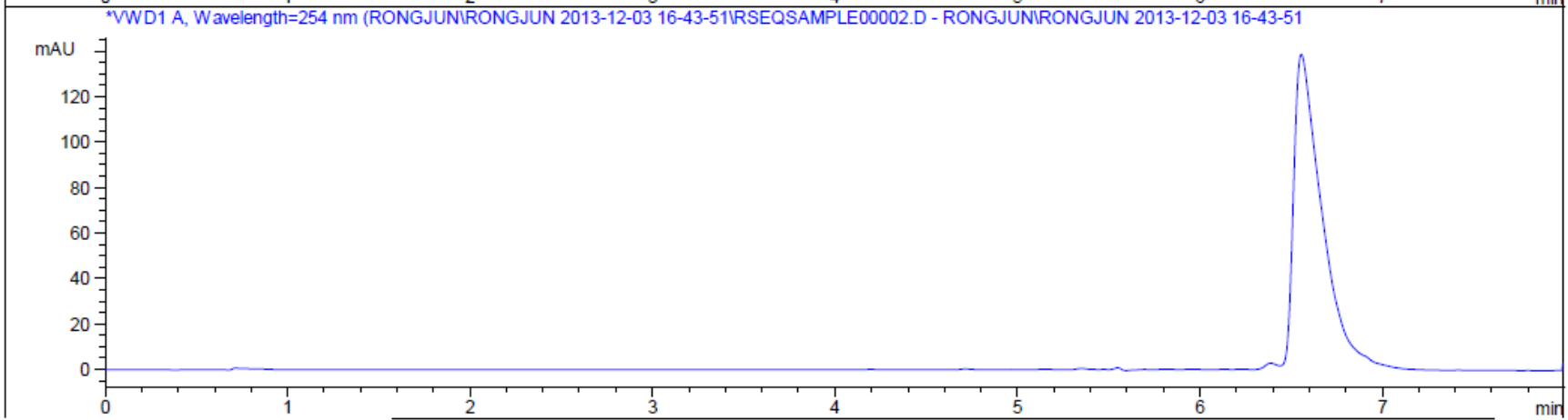
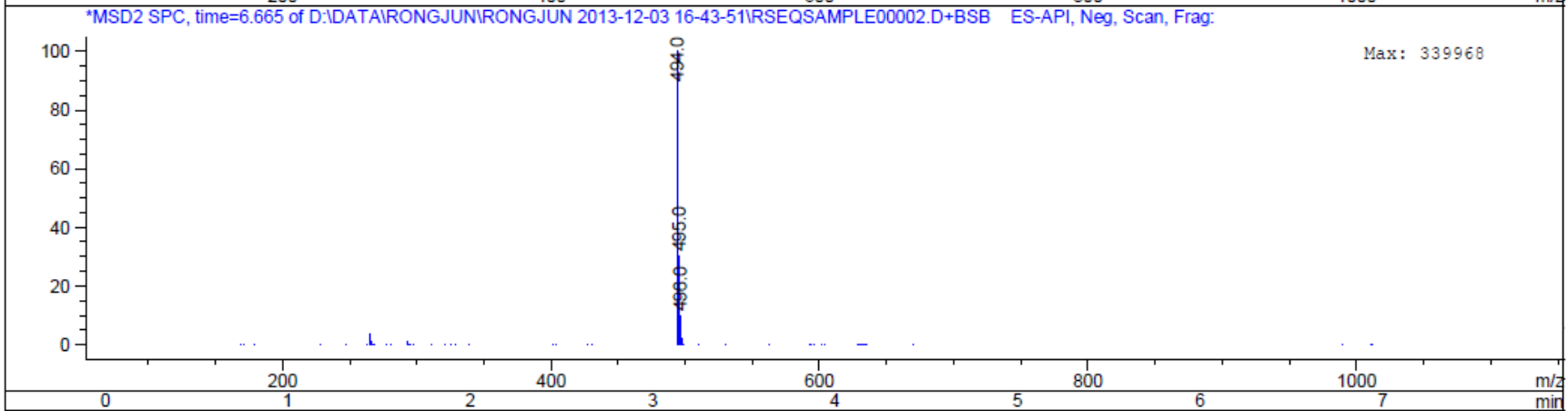
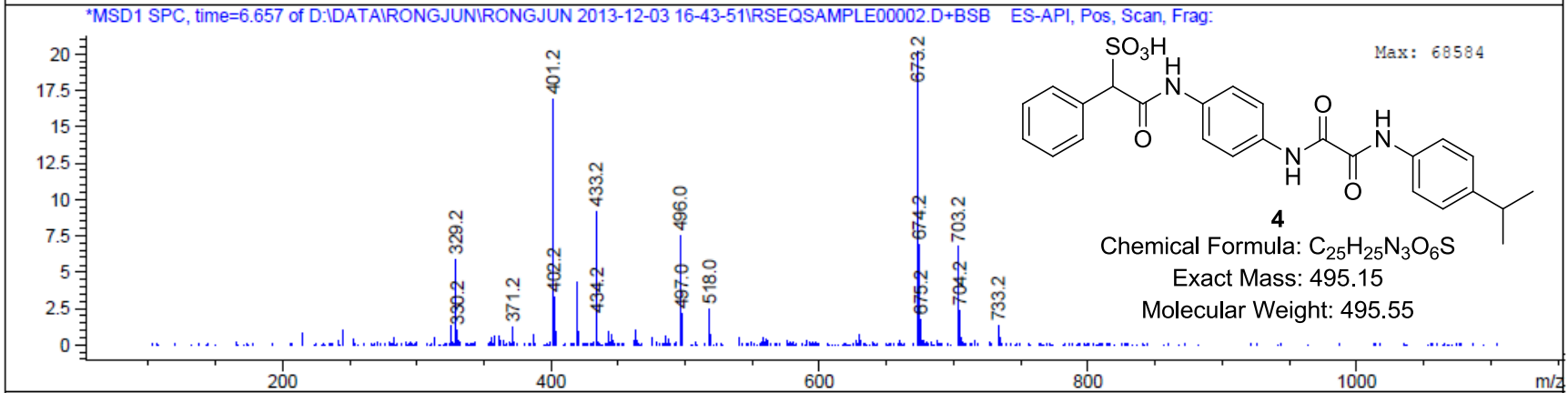


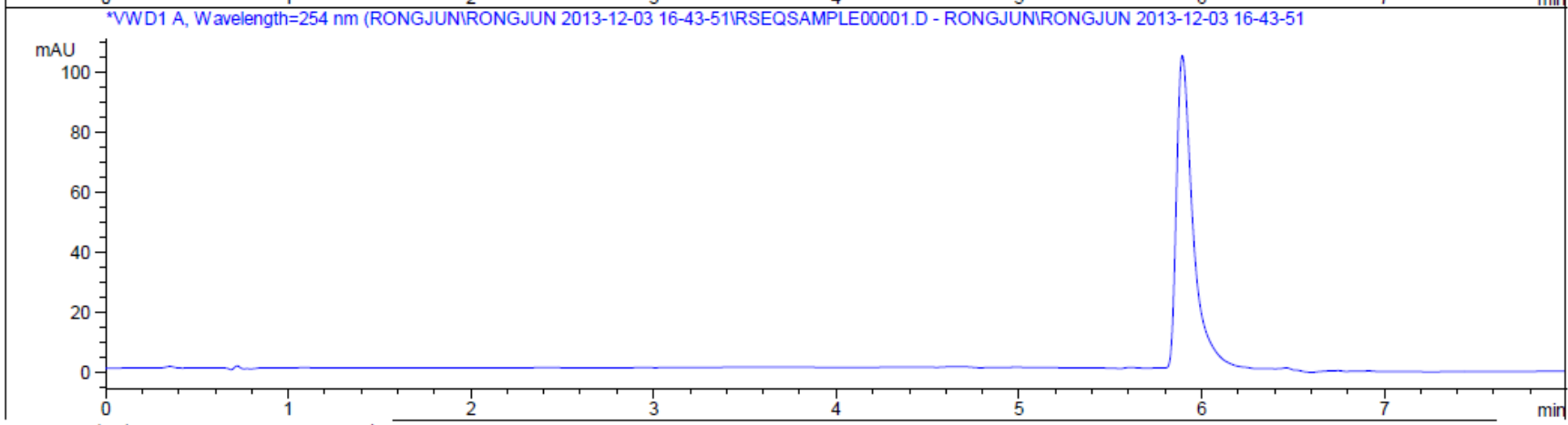
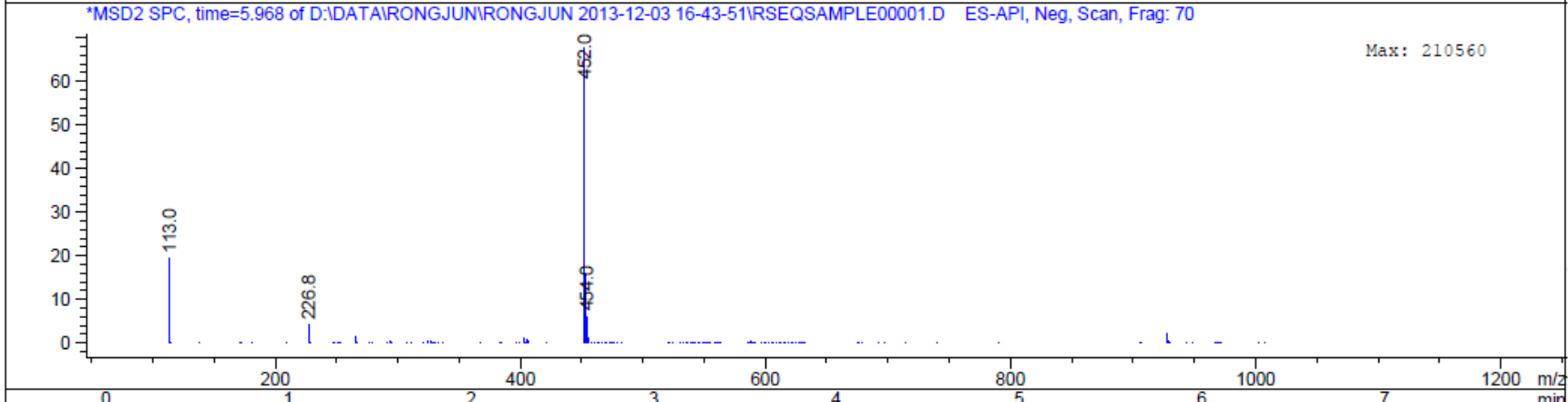
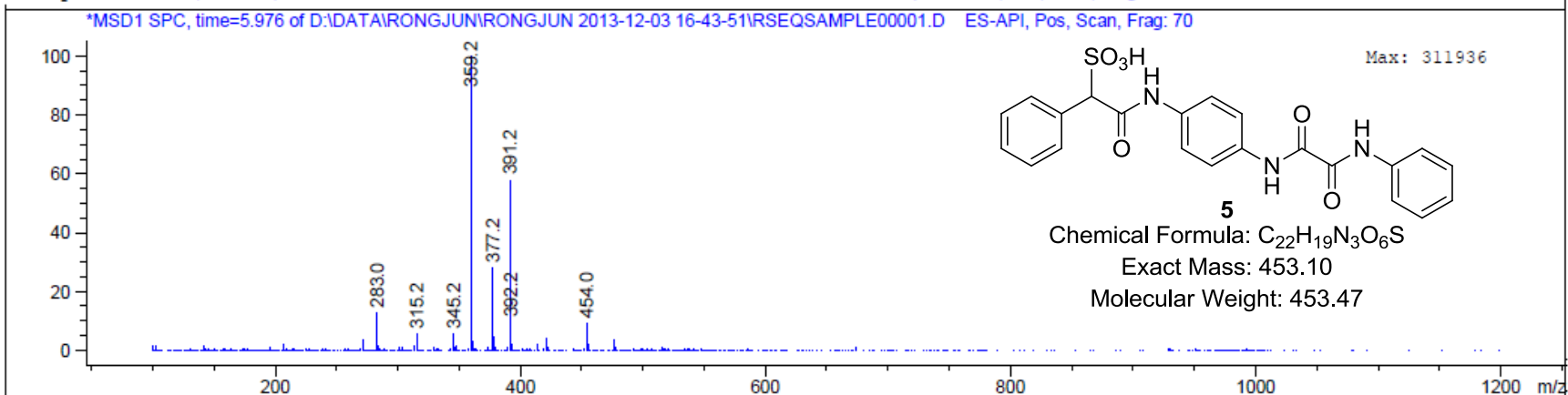


MS Spectrum TIC, MS File (D:\DATA\RONJUN\RONJUN 2013-12-04 14-21-52\RSEQSAMPLE00002.D) ES-API, Pos, Scan, Frag: 70



MS Spectrum TIC, MS File (D:\DATA\RONGJUN\RONGJUN 2013-12-03 16-43-51\RSEQSAMPLE00002.D+BSB) ES-API, Pos, Scan, Frag: 70





13. Experimental Procedures

Protein expression and purification

The SHP2 catalytic domain (residues 224-528) used for kinetic studies and catalytic domain (residues 262-528) used for crystallization were cloned into the pET-21a+ vector using NdeI and XhoI (NEB). These proteins were expressed in *E. coli* BL21(DE3) and purified with Ni-NTA resin (Qiagen). The SHP2 catalytic domain (residues 262-528) was purified by Ni-NTA agarose (Qiagen) followed by sequential chromatography of HiPrep 26 desalting column (GE Healthcare), and cation exchange column packed with SP sepharose (GE Healthcare). Protein purity was determined to be greater than 95% by SDS-PAGE and Coomassie blue staining.

Enzyme kinetics and inhibition studies

The SHP2 phosphatase activity was assayed in 96-well plates using *p*NPP as a substrate at 25°C in 50 mM 3,3-dimethylglutarate (DMG) buffer (pH=7.0), containing 1 mM EDTA with an ionic strength of 0.15 M adjusted by NaCl. The FDA-approved drug collection or the SPAA based libraries were screened in a 96-well format at two different compound concentrations (10 and 20 µM for FDA drugs and 10 and 1 µM for the SPAA libraries). The reaction was initiated by the addition of 50 µl of SHP2 to 150 µl of reaction mixture containing *p*NPP and the compound, the resulting 200 µl mixture has SHP2 at a final concentration of 20 nM, and *p*NPP at a final concentration of 3 mM (the K_m for *p*NPP). The reaction was allowed to proceed for 10 min, and then quenched by addition of 50 µl of 5N NaOH. The amount of product *p*-nitrophenol was determined from the absorbance at 405 nm detected by a Spectra MAX340 microplate spectrophotometer (Molecular Devices) using a molar extinction coefficient of 18,000 M⁻¹cm⁻¹. The nonenzymatic hydrolysis of *p*NPP was corrected by measuring the control without enzyme. The Michaelis-Menten kinetic parameters k_{cat} and K_m were determined from a direct fit of the velocity *versus* substrate concentration data to Michaelis-Menten equation using SigmaPlot program. Inhibitor concentrations used for IC₅₀ measurements cover the range from 0.2 to 5x of the IC₅₀ value. IC₅₀ values for cefsulodin and compounds **2-5** were calculated by fitting the absorbance at 405 nm *versus* inhibitor concentration to the following equation:

$$A_1/A_0=IC_{50}/(IC_{50}+[I])$$

where A_1 is the absorbance at 405 nm of the sample in the presence of inhibitor; A_0 is the absorbance at 405 nm in the absence of inhibitor; and $[I]$ is the concentration of the inhibitor.

For inhibitor selectivity profiling studies, the PTPs, including cytosolic PTPs, SHP1, PTP1B, LYP, HePTP, and Meg2, the receptor-like PTPs, PTP α , PTP β , PTP ϵ , PTP γ , PTP μ and LAR, the dual specificity phosphatases VHR and CDC14A, the low molecular weight (LMW) PTP, and the Ser/Thr protein phosphatase PP5, were expressed and purified from *E. coli*. The inhibition assays for these PTPs were performed under the same conditions as SHP2 except using a different *p*NPP concentration corresponding to the K_m of the PTP studied.

Characterization of cefsulodin-mediated SHP2 inhibition by Q-TOF ESI-MS, LC-MS, and HPLC

Agilent 6520 Accurate-Mass was used for the Q-TOF ESI-MS studies. Water and acetonitrile (both containing 0.1% formic acid) was used as eluent (80% water, flow 50 μ L/min, run time 5 min). ESI positive mode was used with mass range from 300 to 1700, the gas temperature was 325 $^{\circ}$ C, and vaporizer temperature was: 819 $^{\circ}$ C. The sample was adjusted to have a concentration at 0.1 mg/mL, the injection volume of each sample was 1 μ L. Mass hunter software was used for protein deconvolution data analysis to calculate the molecular weight of the protein.

Agilent Technologies 6130 quadrupole LC-MS instrument was used for the LC-MS studies. A C18 reserved phase column (phenomenex, 50 \times 4.6 mm) was used as stationary phase, water and methanol (both containing 0.1% formic acid) was used as mobile phase (gradient: 0-100% methanol, flow 0.8 mL/min, run time 15 min), and UV absorbance at the fixed wavelength of 254 nm and positive and negative ESI-MS data were recorded. The sample was adjusted to have a concentration at 0.1 mg/mL, and the injection volume of each sample was 0.2 μ L. The retention time and corresponding ESI-MS data were used as identity of molecules.

Waters 2545 preparative HPLC purification system was used for compound purification. A C18 reserved phase column (Sunfire, 50 \times 150 mm) was used as stationary phase, water and methanol (both containing 0.1% trifluoroacetic acid) was used as mobile phase (gradient: 0-100% methanol, flow 50

mL/min, run time 60 min), and UV absorbance at the fixed wavelength of 254 nm was used for fraction collection. The compound identity was validated by LC-MS studies following HPLC purification.

X-Ray Crystallography studies

The SHP2•cefsulodin co-crystals were grown at 20°C in the hanging drops containing 1.5 μ L protein solution (8 mg/ml SHP2 with 1 mM cefsulodin in 20 mM MES, pH 5.8, 300 mM NaCl, 2 mM DTT and 1 mM EDTA) and 1.5 μ L reservoir solution (20% PEG3350, 33 mM citric acid, 67 mM BIS-TRIS propane, pH = 7.4). The crystals were transferred into 2 μ L of cryo-protectant buffer (150 mM NaCl, 1 mM cefsulodin, 30% PEG3350, 33 mM citric acid, 67 mM BIS-TRIS propane, pH = 7.4), allowed to soak for 5 min and then flash-frozen by liquid nitrogen. Data were collected at the 19-BM beam line at the Advanced Photon Source (APS) and were processed with HKL3000.⁷ The data were collected to 1.6 Å resolution in the P_{21} space group. The phase was determined by molecular replacement with Molrep⁸ using the coordinates of reported SHP2 structure (PDBID: 3B7O)⁹ as the search model. The SHP2•cefsulodin complex structure was refined using phenix.refine in the PHENIX software suite.¹⁰ The electron density maps were inspected and the model was tuned in Coot.¹¹ The data collection and structure refinements statistics are summarized in Table S1.

Chemical synthesis

Cefsulodin and other antibiotics were used as purchased from Sigma-Aldrich, and all other reagents were from Fisher Scientific. ¹H and ¹³C NMR spectra were obtained on a Bruker Avance II 500 MHz or a Bruker Fourier 300 MHz NMR spectrometer with TMS or residual solvent as standard. Accurate mass data was obtained using an Agilent 6520 Accurate-Mass instrument.

Synthesis of Lib-1, Lib-2, Lib-3, and Lib-4

To α -sulfofenyl acetyl chloride (0.234 g, 1 mmol) and DIEA (0.522 mL, 3 mmol) in DMF (2 mL) was added N-Boc-p-phenylenediamine (0.208 g, 1.0 mmol). The reaction mixture was stirred at rt for 0.5 h and then was concentrated by rotary evaporator. The resulting mixture was treated with 100% TFA at rt for 3 h to remove the Boc protecting group. The mixture was concentrated again by rotary evaporator, and treated with methyl oxalyl chloride (0.135 g, 1.1 mmol) and DIEA (0.522 mL, 3 mmol) in DMF (2 mL) for

0.5 h at rt. Finally the mixture was hydrolyzed by 10% LiOH to furnish product 2-oxo-2-((4-(2-phenyl-2-sulfoacetamido)phenyl)amino)acetic acid (**Lib-1**). Subsequently it was subjected to HPLC purification, and product **Lib-1** was obtained as colorless oil with 56% overall yield and >95% purity. 2-oxo-2-((3-(2-phenyl-2-sulfoacetamido)phenyl)amino)acetic acid (**Lib-2**) and 2-oxo-2-((4-(2-phenyl-2-sulfoacetamido)benzyl)amino)acetic acid (**Lib-3**) were obtained in similar procedures by using N-Boc-m-phenylenediamine and 4-[(N-Boc)aminomethyl]aniline, respectively. 2-oxo-2-((4-((2-phenyl-2-sulfoacetamido)methyl)phenyl)amino)acetic acid (**Lib-4**) was synthesized in slightly different procedure. 4-[(N-Boc)aminomethyl]aniline was treated with methyl oxalyl chloride (0.135 g, 1.1 mmol) and DIEA (0.522 mL, 3 mmol) in DMF (2 mL) for 0.5 h at rt. The mixture was concentrated and then treated with 100% TFA at rt for 3 h to remove the Boc protecting group. The crude mixture was concentrated by rotary evaporator and treated with α -sulfofenyl acetyl chloride (0.257 g, 1.1 mmol) and DIEA (0.522 mL, 3 mmol) in DMF (2 mL). The mixture was finally hydrolyzed by 10% LiOH and subjected to HPLC purification, and product 2-oxo-2-((4-((2-phenyl-2-sulfoacetamido)methyl)phenyl)amino)acetic acid (**Lib-4**) was obtained as colorless oil in 82% overall yield with >90% purity.

2-oxo-2-((4-(2-phenyl-2-sulfoacetamido)phenyl)amino)acetic acid (**Lib-1**): ^1H NMR (500 MHz, DMSO-*d*₆) δ 10.65 (s, 1H), 10.31(s, 1H), 7.69 (d, $J = 9.1$ Hz, 2H), 7.57-7.54(m, 4H), 7.30-7.24 (m, 3H), 4.75 (s, 1H). ^{13}C NMR (125 MHz, DMSO-*d*₆) δ 165.8, 162.2, 156.6, 135.8, 135.3, 133.0, 129.9, 127.4, 127.0, 71.8. ESI-MS Calcd. for C₁₆H₁₃N₂O₇S (M-H⁺): m/z 377.0449; found 377.0450.

2-oxo-2-((3-(2-phenyl-2-sulfoacetamido)phenyl)amino)acetic acid (**Lib-2**): ^1H NMR (500 MHz, DMSO-*d*₆) δ 10.68 (s, 1H), 10.36 (s, 1H), 8.03 (t, $J = 1.6$ Hz, 1H), 7.57-7.55 (m, 2H), 7.44-7.38 (m, 2H), 7.30-7.24 (m, 4H), 4.78 (s, 1H). ^{13}C NMR (125 MHz, DMSO-*d*₆) δ 166.0, 162.2, 157.0, 139.4, 138.0, 135.2, 129.9, 129.0, 127.5, 127.0, 115.4, 115.3, 111.1, 71.8. ESI-MS Calcd. for C₁₆H₁₃N₂O₇S (M-H⁺): m/z 377.0449; found 377.0445.

2-oxo-2-((4-(2-phenyl-2-sulfoacetamido)benzyl)amino)acetic acid (**Lib-3**): ^1H NMR (500 MHz, DMSO-*d*₆) δ 10.30 (s, 1H), 9.31 (t, $J = 6.2$ Hz, 1H), 7.56-7.51 (m, 4H), 7.29-7.19 (m, 5H), 4.74 (s, 1H), 4.26 (d, $J = 6.3$ Hz, 2H). ^{13}C NMR (125 MHz, DMSO-*d*₆) δ 165.9, 162.2, 158.4, 138.0, 135.3, 133.3, 129.9,

127.9, 127.5, 127.0, 118.9, 71.8, 30.7. ESI-MS Calcd. for C₁₇H₁₅N₂O₇S (M-H⁺): m/z 391.0605; found 391.0609.

2-oxo-2-((4-((2-phenyl-2-sulfoacetamido)methyl)phenyl)amino)acetic acid (**Lib-4**): ¹H NMR (500 MHz, DMSO-*d*₆) δ 10.68 (s, 1H), 8.64 (t, *J* = 5.9 Hz, 1H), 7.68 (d, *J* = 8.6 Hz, 2H), 7.49-7.48 (m, 2H), 7.29-7.24 (m, 5H), 4.55 (s, 1H), 4.31 (dd, *J* = 5.9, 11.1 Hz, 2H). ¹³C NMR (125 MHz, DMSO-*d*₆) δ 167.5, 162.2, 156.7, 136.3, 135.6, 135.6, 129.7, 127.4, 127.3, 126.8, 120.2, 71.5, 30.7. ESI-MS Calcd. for C₁₇H₁₅N₂O₇S (M-H⁺): m/z 391.0605; found 391.0599.

SPAA-based library synthesis

To all wells of 96-well plates were added 2-oxo-2-((4-(2-phenyl-2-sulfoacetamido)phenyl)amino)acetic acid (**Lib-1**) (20 μL, 20 mM in DMF), HBTU (20 μL, 20 mM in DMF), HOBt (20 μL, 20 mM in DMF), DIEA (20 μL, 60 mM in DMF), and corresponding 192 amines from storage plates (1.2 μL, 0.5 mM in DMF), the reaction plates were placed at rt for 1 day. Compounds from 2-oxo-2-((3-(2-phenyl-2-sulfoacetamido)phenyl)amino)acetic acid (**Lib-2**), 2-oxo-2-((4-(2-phenyl-2-sulfoacetamido)benzyl)amino)acetic acid (**Lib-3**) and 2-oxo-2-((4-((2-phenyl-2-sulfoacetamido)methyl)phenyl)amino)acetic acid (**Lib-4**) were synthesized by the same procedure. The reaction wells from aniline were monitored by LC-MS to show that reactions occurred well in great conversions. The libraries were made as racemic mixtures. Four libraries of 768 compounds were obtained with estimated concentration at 4 mM (assuming 80% product yield), which was screened against PTPs as described.

Synthesis of compounds 2-5.

To 2-oxo-2-((4-(2-phenyl-2-sulfoacetamido)phenyl)amino)acetic acid (**Lib-1**) (0.0756 g, 0.2 mmol) in DMF (2 mL) was added HBTU (0.078 g, 0.2 mmol), HOBt (0.031 g, 0.2 mmol), DIEA (0.105 mL, 0.6 mmol), and 4-iodoaniline (0.053 g, 0.22 mmol) sequentially, and the reaction mixture was stirred at rt for 1 h. The mixture was then subjected to HPLC purification, and product 2-((4-(2-((4-iodophenyl)amino)-2-oxoacetamido)phenyl)amino)-2-oxo-1-phenylethanesulfonic acid (**2**) was obtained as colorless oil (97% yield, >95% purity). Products **3** to **5** were obtained in the same manner. The products compounds 2-5 are stable, and no degradation was observed in LC-MS spectra after 1 year storage in DMS at 4 °C.

2-((4-(2-((4-iodophenyl)amino)-2-oxoacetamido)phenyl)amino)-2-oxo-1-phenylethanesulfonic acid (compound **2**): ¹H NMR (500 MHz, DMSO-*d*₆) δ 10.91 (s, 1H), 10.77 (s, 1H), 10.33 (s, 1H), 7.78 (d, *J* = 8.9 Hz, 2H), 7.73-7.68 (m, 4H), 7.60-7.58 (m, 4H), 7.30-7.25 (m, 3H), 4.78 (s, 1H). ¹³C NMR (125 MHz, DMSO-*d*₆) δ 165.9, 158.9, 158.1, 137.6, 137.4, 135.8, 135.2, 132.8, 129.9, 127.4, 126.9, 122.6, 120.9, 119.1, 88.7, 71.8. ESI-MS Calcd. for C₂₂H₁₇N₃O₆S (M-H⁺): *m/z* 577.9888; found 577.9883.

2-((4-(2-([1,1'-biphenyl]-4-ylamino)-2-oxoacetamido)phenyl)amino)-2-oxo-1-phenylethanesulfonic acid (compound **3**): ¹H NMR (300 MHz, DMSO-*d*₆) δ 10.92 (s, 1H), 10.81(s, 1H), 10.31 (s, 1H), 7.96-7.26 (m, 18H), 4.72 (s, 1H). ESI-MS Calcd. for C₂₈H₂₂N₃O₆S (M-H⁺): *m/z* 528.1235; found 528.1231.

2-((4-(2-((4-isopropylphenyl)amino)-2-oxoacetamido)phenyl)amino)-2-oxo-1-phenylethanesulfonic acid (compound **4**): ¹H NMR (300 MHz, DMSO-*d*₆) δ 10.78 (s, 1H), 10.74 (s, 1H), 10.33 (s, 1H), 7.80-7.73 (m, 4H), 7.59-7.56 (m, 4H), 7.25-7.22 (m, 5H), 4.73 (s, 1H), 2.91-2.82 (m, 1H), 1.19 (d, *J* = 9.0 Hz, 6H). ESI-MS Calcd. for C₂₅H₂₄N₃O₆S (M-H⁺): *m/z* 494.1391; found 494.1394.

2-oxo-2-((4-(2-oxo-2-(phenylamino)acetamido)phenyl)amino)-1-phenylethanesulfonic acid (compound **5**): ¹H NMR (300 MHz, DMSO-*d*₆) δ 10.80 (s, 2H), 10.34 (s, 1H), 7.87-7.78 (m, 4H), 7.60-7.56 (m, 4H), 7.40-7.27 (m, 6H), 4.78 (s, 1H). ¹³C NMR (75 MHz, DMSO-*d*₆) δ 166.3, 159.2, 158.8, 138.1, 136.3, 135.6, 133.4, 130.3, 129.2, 127.9, 127.4, 125.1, 121.3, 120.9, 119.6, 72.1. ESI-MS Calcd. for C₂₂H₁₈N₃O₆S (M-H⁺): *m/z* 452.0922; found 452.0917.

Cell proliferation and immunoblot analysis

Human non-small cell lung carcinoma cell line H1975 was cultured at 37 °C and 5% CO₂ in RPMI-1640 (Corning) supplemented with 10% fetal bovine serum (HyClone). Human breast cancer cell line MDA-MB-231 was cultured in DMEM supplemented with 10% fetal bovine serum. For cell proliferation assay, 2~3×10³ cells were seeded in each well of 96-well plates. After treating cells with compounds for 2 days, cells were incubated with 50 ng/ml MTT (3-(4,5-Dimethylthiazol-2-yl)-2,5-diphenyltetrazolium bromide) for 3~4 hours. Then the culture medium was removed, DMSO was added to dissolve the formazan crystals. Wells containing only media were used for background correction. The optical density

was measured spectrophotometrically at 540 nm. For signaling analysis, cells were serum-starved overnight followed by treatment with vehicle or compounds for 3 hours, and then either left un-stimulated or stimulated with 5 ng/ml EGF or 10 nM PMA (Sigma) for indicated time. Cells were lysed and the lysates were electrophoresed on a 10% polyacrylamide gel, and then transferred to a nitrocellulose membrane, and probed with anti-phospho-ERK1/2 and anti-ERK1/2 (Cell Signaling) antibodies followed by incubation with horseradish peroxidase-conjugated secondary antibodies. The blots were developed by the enhanced chemiluminescence technique using the SuperSignal West Pico Chemiluminescent substrate (Pierce).

Effects of compound 2 on cell growth in Matrigel

Approximately 300,000 SKBR3 cells were seeded into 150 μ L of growth factor reduced Matrigel (BD) that was then covered with 2 mLs of media containing either 20 μ L vehicle (DMSO) or the indicated concentrations of compound **2**. Cells were then imaged at 24 hours intervals using a NIKON SMZ1500 stereomicroscope. After 5 days the cells were recovered from the Matrigel by the following method. Media was aspirated and cells were washed with 500 μ L of cold PBS. 150 μ L of RIPA lysis buffer supplemented with ProteCEASE-50, EDTA Free protease inhibitors (GBiosciences) was added to the Matrigel. Cells were scraped into a slurry and instantly frozen using dry ice for 5 minutes. After thawing tubes were spun down at 4°C for 10 minutes at 14K rpm. Proteins were then resolved by SDS-PAGE and the relative levels of total and phospho-ERK1/2 were detected by immunoblot analysis.

14. References

- (1) Zhang, Z. Y. Protein tyrosine phosphatases: prospects for therapeutics. *Curr. Opin. Chem. Biol.* **2001**, *5*, 416-423.
- (2) Liu, S. J.; Zhou, B.; Yang, H. Y.; He, Y. T.; Jiang, Z. X.; Kumar, S.; Wu, L.; Zhang, Z. Y. Aryl vinyl sulfonates and sulfones as active site-directed and mechanism-based probes for protein tyrosine phosphatases. *J. Am. Chem. Soc.* **2008**, *130*, 8251-8260.
- (3) Fujita, T.; Koshiro, A. Kinetics and mechanism of the degradation and epimerization of sodium cefsulodin in aqueous solution. *Chem. Pharm. Bull.* **1984**, *32*, 3651-3661.
- (4) Deshpande, A. D.; Baheti, K. G.; Chatterjee, N. R. Degradation of beta-lactam antibiotics. *Curr. Sci.* **2004**, *87*, 1684-1695.
- (5) Perez-Inestrosa, E.; Suau, R.; Montanez, M. I.; Rodriguez, R.; Mayorga, C.; Torres, M. J.; Blanca, M. Cephalosporin chemical reactivity and its immunological implications. *Current Opinion in Allergy and Clinical Immunology* **2005**, *5*, 323-330.
- (6) Nomura, H.; Fugono, T.; Hitaka, T.; Minami, I.; Azuma, T.; Morimoto, S.; Masuda, T. Semisynthetic beta-lactam antibiotics. 6. 1 Sulfocephalosporins and their antipseudomonal activities. *Journal of Medicinal Chemistry* **1974**, *17*, 1312-5.
- (7) Otwinowski, Z.; Minor, W. Processing of X-ray diffraction data collected in oscillation mode. In *Macromolecular Crystallography, Pt A*, Academic Press Inc: San Diego, 1997; Vol. 276, pp 307-326.
- (8) Vagin, A.; Teplyakov, A. MOLREP: an automated program for molecular replacement. *J. Appl. Crystallogr.* **1997**, *30*, 1022-1025.
- (9) Barr, A. J.; Ugochukwu, E.; Lee, W. H.; King, O. N. F.; Filippakopoulos, P.; Alfano, I.; Savitsky, P.; Burgess-Brown, N. A.; Muller, S.; Knapp, S. Large-scale structural analysis of the classical human protein tyrosine phosphatome. *Cell* **2009**, *136*, 352-363.
- (10) Adams, P. D.; Afonine, P. V.; Bunkoczi, G.; Chen, V. B.; Davis, I. W.; Echols, N.; Headd, J. J.; Hung, L. W.; Kapral, G. J.; Grosse-Kunstleve, R. W.; McCoy, A. J.; Moriarty, N. W.; Oeffner, R.; Read, R. J.; Richardson, D. C.; Richardson, J. S.; Terwilliger, T. C.; Zwart, P. H. PHENIX: a comprehensive Python-based system for macromolecular structure solution. *Acta Crystallogr. Sect. D-Biol. Crystallogr.* **2010**, *66*, 213-221.
- (11) Emsley, P.; Lohkamp, B.; Scott, W. G.; Cowtan, K. Features and development of Coot. *Acta Crystallogr. Sect. D-Biol. Crystallogr.* **2010**, *66*, 486-501.